

A Survey on Bridging EEG Signals and Generative AI: From Image and Text to Beyond

Shreya Shukla, Jose Torres, Akshaj Murhekar, Christina Liu, Abhijit Mishra, Jacek Gwizdka, Shounak Roychowdhury

School of Information, The University of Texas at Austin, Austin, TX, USA

Abstract

Decoding neural activity into human-interpretable representations is a key research direction in brain-computer interfaces (BCIs) and computational neuroscience. Recent progress in machine learning and generative AI has driven growing interest in transforming non-invasive Electroencephalography (EEG) signals into images, text, and audio. This survey consolidates and analyzes developments across EEG-to-image synthesis, EEG-to-text generation, and EEG-to-audio reconstruction. We conducted a structured literature search across major databases (2017-2025), extracting key information on datasets, generative architectures (GANs, VAEs, transformers, diffusion models), EEG feature-encoding techniques, evaluation metrics, and the major challenges shaping current work in this area. Our review finds that EEG-to-image models predominantly employ encoder-decoder architectures built on GANs, VAEs, or diffusion models; EEG-to-text approaches increasingly leverage transformer-based language models for open-vocabulary decoding; and EEG-to-audio methods commonly map EEG signals to mel-spectrograms that are subsequently rendered into audio using neural vocoders. Despite promising advances, the field remains constrained by small and heterogeneous datasets, limited cross-subject generalization, and the absence of standardized benchmarks. By consolidating methodological trends and available datasets, this survey provides a foundational reference for advancing EEG-based generative AI and supporting reproducible research. We further highlight open-source datasets and baseline implementations to facilitate systematic benchmarking and accelerate progress in EEG-driven neural decoding.

Keywords: EEG, Generative AI, Electroencephalography, EEG to Text, EEG to Image, EEG to Audio, neural signals, generation

1. Introduction & Motivation

The convergence of Brain-Computer Interfaces (BCIs) and Generative Artificial Intelligence (GenAI) is opening a transformative path toward direct brain-to-device communication. Advances in human-computer interaction have already supported applications in assistive communication for individuals with disabilities, cognitive neuroscience, mental health assessment, augmented and virtual reality (AR/VR), and neural art generation. Although invasive and minimally invasive BCIs are beginning to show real viability for industrial deployment, non-invasive systems remain comparatively underdeveloped and are still mostly confined to academic research and prototypes. Their broader adoption is constrained by the lower spatial and temporal resolution of different non-invasive signals, which presents significant challenges. These constraints highlight the need to examine recent progress in generative methods for non-invasive neural data in order to clarify emerging methodologies, identify current limitations, and opportunities for advancement in this domain.

Among non-invasive neural recording techniques such as functional Magnetic Resonance Imaging (fMRI), Electroen-

cephalography (EEG), and Magnetoencephalography (MEG), this survey primarily focuses on EEG. EEG measures the brain's electrical activity from the scalp, providing high temporal resolution that enables detection of rapid neural changes at the millisecond scale. Figure 1 illustrates the EEG acquisition process: electrical signals generated by neural activity are captured using headsets equipped with 12-256 electrodes (or channels) while participants are exposed to external stimuli such as images, text, or audio. These electrodes are spatially mapped to specific cortical regions, enabling localized observation of brain responses. While EEG has lower spatial resolution compared to fMRI or MEG, numerous studies demonstrate that it can still capture distinct activity patterns across different cortical regions in response to various stimuli (Lutzenberger et al., 1995; Pfurtscheller et al., 1994; Khadir et al., 2023; Bastiaansen et al., 2008; Marinković, 2004). EEG serves as a key neuro-physiological tool for assessing brain activity, particularly within the cerebral cortex, which is organized into four major lobes: **frontal, temporal, parietal, and occipital**, shown in Figure 1(a). The frontal lobe is associated with higher cognitive functions and decision-making; the temporal lobe plays a primary role in auditory processing and multimodal sensory integration; the parietal lobe is involved in attention and language-related processes; and the occipital lobe processes visual information.

EEG signals are inherently **spatiotemporal**, consisting of a temporal component that reflects dynamic neural oscillations

Email addresses: shreya.shukla@utexas.edu (Shreya Shukla), jtorres1221@utexas.edu (Jose Torres), akshaj.murhekar@utexas.edu (Akshaj Murhekar), c149786@utexas.edu (Christina Liu), abhijitmishra@utexas.edu (Abhijit Mishra), jacekg@utexas.edu (Jacek Gwizdka), shounak.roychowdhury@utexas.edu (Shounak Roychowdhury)

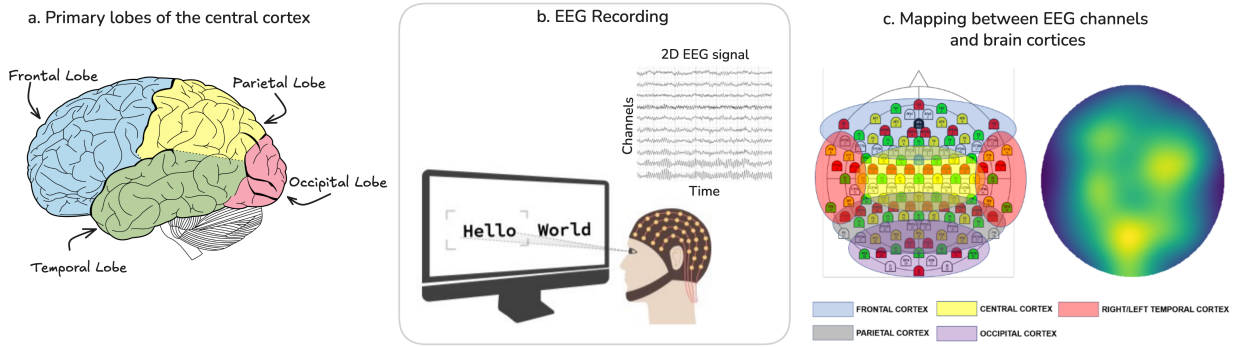


Figure 1: (a) Diagram of the primary lobes of cerebral cortex, including frontal, parietal, temporal, and occipital, highlighting their anatomical boundaries.(b) EEG Recording: Illustration of EEG activity recorded while participants view text stimuli, showing eye-gaze position and a 2-dimensional representation of the corresponding EEG signals. (c) Mapping between EEG channels and brain cortices: On the left is the visualization of each electrode in the 128-Channel EEG electrode placement mapped to a specific cortical region, with mappings shown across frontal, central, temporal, parietal, and occipital cortices. On the right is the neural activation visualization taken from the top of the scalp (Palazzo et al., 2020).

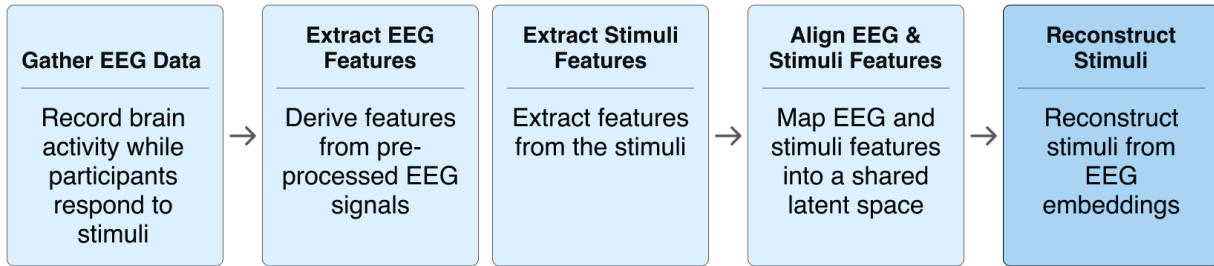


Figure 2: General Steps from EEG Data Gathering to Stimuli Reconstruction (Image, Text, or Audio)

and a spatial component defined by the configuration of electrodes across the scalp. Typical EEG amplitudes range from 2–500 μV and frequencies from 1–100 Hz. These signals are conventionally grouped into five frequency bands: δ (delta, 0.5–4 Hz), θ (theta, 4–7 Hz), α (alpha, 8–12 Hz), β (beta, 13–30 Hz), and γ (gamma, 30–100 Hz). Throughout this survey, we use these symbols and band names interchangeably.

Traditionally, researchers have investigated the synchronization and desynchronization of EEG rhythms across these bands to understand how neural activity changes in response to cognitive engagement or external stimuli (Pfurtscheller et al., 1994; Krause et al., 1996, 1997). Synchronization occurs when oscillations across cortical regions become more coordinated and rhythmic, often reflecting an idle or resting state with reduced information processing. Desynchronization, in contrast, reflects a reduction in rhythmic coherence and is typically associated with active cortical engagement during sensory or cognitive tasks. These changes in oscillatory activity across frequency bands provide a window into large-scale neural dynamics in response to stimuli (Marinković, 2004; Bastiaansen et al., 2008; Weiss et al., 2005; Lutzenberger et al., 1995; Pfurtscheller et al., 1994), and may contain decodable traces of perceptual, cognitive, and semantic representations.

We hypothesize that frequency-specific and region-specific oscillatory patterns enrich the information content available in EEG signals, thereby enabling EEG-to-media generation models to decode and reconstruct underlying per-

ceptual, cognitive, and semantic representations. Building on this hypothesis, and given that EEG supports both passive and active Brain-Computer Interface (BCI) paradigms, it holds significant potential for **adaptive human-computer interaction** (Zander et al., 2010; Wolpaw and Boulay, 2010).

In light of recent breakthroughs in Generative AI, this survey presents a comprehensive review of advances in **EEG-based cross-modal generation**, focusing on two primary directions. The first is **EEG-to-image generation**, which involves the generation and reconstruction of visual stimuli from brain signals by leveraging models such as *Generative Adversarial Networks (GANs)* and *Diffusion Models* (Goodfellow et al., 2020; Ho et al., 2020) to decode visual perception. The second direction explores **EEG-to-text translation**, where *Recurrent Neural Networks (RNNs)* and *Transformer-based language models* (Vaswani et al., 2017) are employed to learn and generate linguistic representations from neural activity. Beyond these two main lines of research, this survey also discusses emerging efforts in **audio/speech decoding from EEG signals** and multi-modal integration, where the stimuli presented to subjects and the generated media belong to different modalities.

We highlight in Figure 2 a high-level overview of the EEG-to-stimuli generation pipeline, illustrating the **key stages from neural data acquisition to the generation of text, images, or audio**, serving as a conceptual starting point for the survey. The survey is organized into three main sections: EEG-to-Image, EEG-to-Text, and EEG-to-Audio/Speech generation,

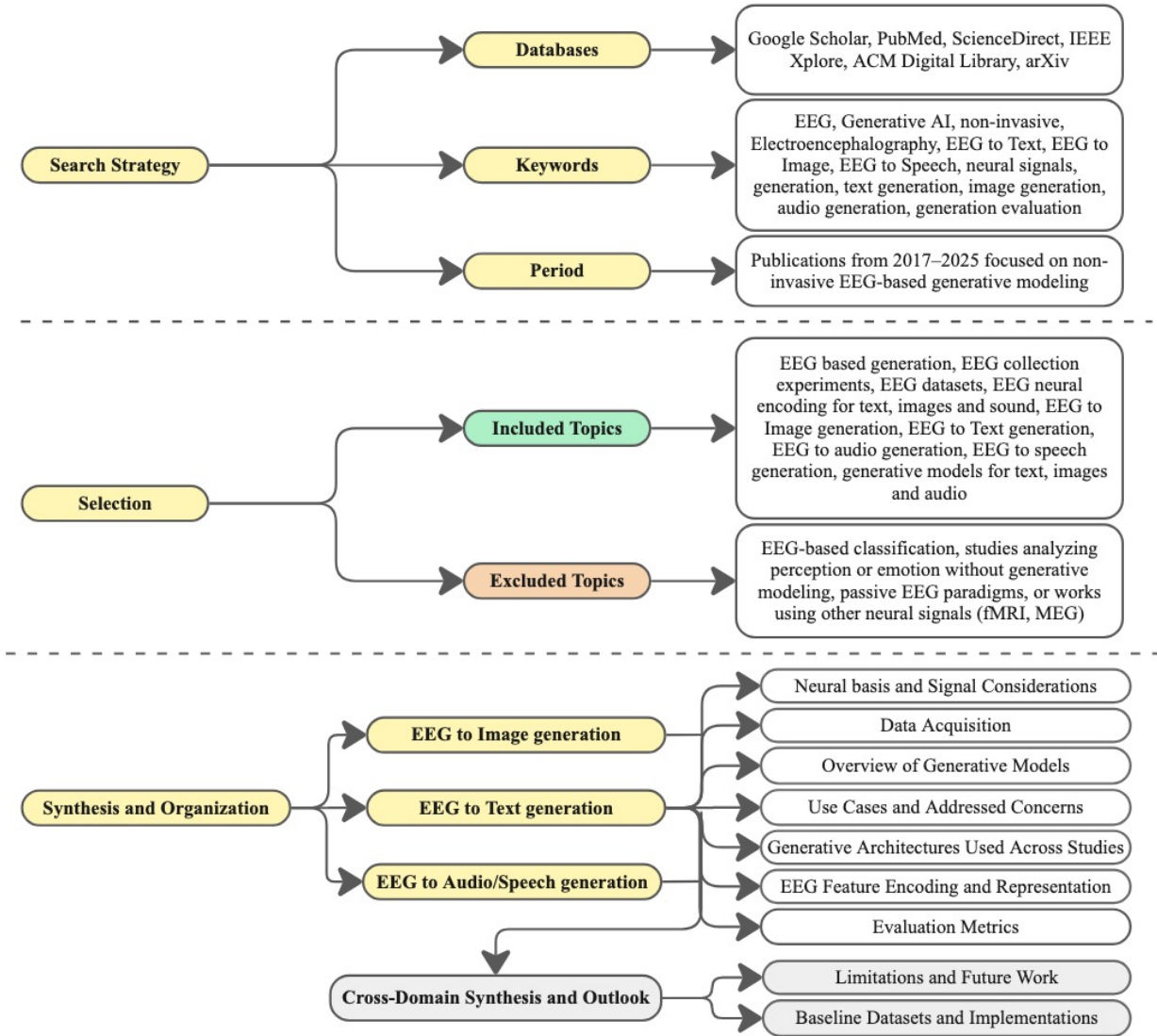


Figure 3: Overview of the literature search, selection, and synthesis framework for this topical review. The upper tiers summarize the search strategy and inclusion criteria for EEG-based generative modeling studies. The synthesis and organization tier maps to modality-specific sections (EEG-to-image, EEG-to-text, and EEG-to-audio/speech generation), each analyzed through dimensions such as neural basis, generative architectures, challenges tackled by studies, and evaluation methods. The cross-domain synthesis and outlook section integrates future research directions and suggested baseline implementations for practitioners.

with each section progressing in a linear and structured manner. Because survey papers can be conceptually dense, **we encourage readers to follow the sections in order for a coherent understanding of the field.** We first outline the neural basis of EEG responses to different modalities, describing the relevant cortical regions, how EEG captures their activity, and the dominant frequency bands involved. Next, we summarize data collection procedure and highlight the characteristics of datasets used across the literature. We then provide an overview of foundational Generative AI methodologies to establish the technological context for interpreting the studies that follow. The modality-specific sections then review the use cases examined in prior work, the challenges addressed, the generative architectures, EEG feature-encoding techniques employed, and the reported evaluation metrics.

Finally, we discuss the limitations identified across studies, propose future research directions, and highlight baseline datasets and implementations in [Appendix A](#) that can support reproducibility and enable systematic tracking of progress in the field. By consolidating these developments, this survey aims to provide researchers and practitioners with a cohesive understanding of EEG-based generative AI and its potential to expand the frontiers of **brain-computer interaction.**

2. Method

To capture the breadth of work at the intersection of EEG and generative AI, we conducted a literature search across multiple indexing services, including Google Scholar, PubMed, ScienceDirect, IEEE Xplore, ACM Digital Library, and arXiv.

Search strings combined terms such as “*EEG*,” “*Electroencephalography*,” “*text generation*,” “*image reconstruction*,” “*speech synthesis*,” and “*generative AI*.” These terms were iteratively refined to capture studies across different modalities and architectures. In Figure 3, we present a flowchart outlining the search strategy, selection criteria, and organizational synthesis of the reviewed studies and associated technologies. Our primary focus was on work published between 2017 and 2025, reflecting the period during which deep learning and generative modeling have driven most advances in this field. Studies were included if they used non-invasive EEG signals and applied machine learning or generative AI approaches to produce cross-modal outputs such as text, images, or audio. We considered both peer-reviewed publications and influential preprints. Excluded works included those that focused exclusively on classification tasks (e.g., sentiment analysis, motor imagery recognition, emotion recognition), used other non-invasive techniques like functional magnetic resonance imaging (fMRI), magnetoencephalography (MEG) or invasive neural recordings as these fall outside the scope of EEG-based generative modeling.

For each selected study, we compiled structured notes in tabular form, which had the investigated modality (image, text, audio or speech), study use case, addressed challenges, model architectures employed by studies (e.g., GANs, VAEs, transformers, diffusion models), EEG feature encoding strategies, datasets used and reported evaluation metrics. These tables provided a consistent framework to compare studies and enabled us to identify patterns across the literature. We then grouped studies into three major categories of EEG-driven generation—image, text, and audio—and within each modality, analyzed use cases, architectures, encoding techniques, and evaluation practices. This organization allowed us to highlight both common challenges and emerging trends.

Additionally, for the **foundational knowledge** required to interpret the reviewed studies, we also include background on the neural basis of EEG responses to different stimuli and an overview of generative methods used across modalities. Our goal overall is to provide a balanced, comprehensive and structured overview, ensuring that readers can follow how different approaches have been applied, what challenges they help overcome, existing limitations, and the future direction for further progress in this field.

3. EEG-to-Image Generation

3.1. Neural Basis and Signal Considerations

In EEG-based generation studies, the underlying neural basis is often overlooked, which we believe is essential to motivate how perceptual, semantic, and auditory information can be reconstructed from the recorded signals.

EEG has long been used as a tool to study visual perception. An early study by [Lutzenberger et al. \(1995\)](#) investigates the effect of visual field presentation by changing the stimulus position in the upper versus lower visual field. The authors found that coherent stimuli in the upper visual field, which is

processed by the lower half of the retina and thus the more ventral (lower) sites of the primary visual cortex, elicited a **40 Hz spectral power enhancement over lower occipital electrodes**. Conversely, stimuli presented in the lower visual field produced a corresponding enhancement over upper occipital electrodes. These findings demonstrate that EEG can reliably capture location-specific cortical responses to visual stimuli.

Beyond this, EEG has been extensively used to understand the broader dynamics of visual perception. Cognitive activity in response to visual stimuli unfolds through successive stages, including primary visual processing, feature extraction, higher-level cognitive analysis, and attentional modulation. Although early visual processing is primarily associated with occipital regions, EEG studies consistently show that visual processing engages a broader network spanning occipito-parietal, and frontal areas as information progresses from low-level sensory analysis to higher-order cognitive interpretation. To understand the **timing** (relative to stimulus onset) and **spatial distribution** (across cortical regions) of these processes, researchers commonly examine **changes in oscillatory activity across EEG frequency bands**, such as event-related desynchronization (ERD), along with visual evoked potentials (VEPs), which reflect electrical responses originating in the visual cortex.

ERD in the **alpha band** serves as a well-established marker of cortical activation: while high alpha amplitude is characteristic of a resting or “idle” state, a reduction in alpha power (desynchronization) indicates a change from a resting to an activated state. A foundational study by [Pfurtscheller et al. \(1994\)](#) analyzed ERD in alpha sub-bands during visual processing and identified two distinct components: (i) a **short-lasting upper-alpha (10-12 Hz) desynchronization** localized over **occipital regions**, and (ii) a **longer-lasting lower-alpha (6-8 Hz) desynchronization** that is more broadly distributed, with maximal effects over **parietal areas**. The occipital ERD component peaks approximately **200-300 ms after stimulus onset**, whereas the parietal component reaches its maximum around 300-500 ms, reflecting the progression from early visual analysis to broader cognitive engagement. These temporal and spatial patterns, observed through EEG, provide a useful way to **trace how visual information propagates through cortical networks**.

Cross-frequency interactions also play a role in visual perception. Another study by [Demiralp et al. \(2007\)](#) examined the interaction between theta and gamma oscillations during visual perception using EEG. They found that event-related gamma activity was strongly dependent on the phase of concurrent theta oscillations, indicating that **theta rhythms modulate gamma-band responses**. This cross-frequency coupling is believed to play an important role in perceptual and cognitive processes, including **visual perception**. In their findings, gamma activity was primarily localized over the occipital cortex, whereas theta activity was more broadly distributed, extending into frontal regions, highlighting the **integration of localized sensory processing in response to visual stimuli, with more widespread cognitive networks**.

EEG studies have also examined how oscillatory activity varies with **color perception**. [Khadir et al. \(2023\)](#) analyzed theta, alpha, beta, and gamma oscillations across occipital,

Dataset	Reference	Stimuli Type	Channels /Electrodes	Stimuli Details	Subjects
Zuco 1.0	Hollenstein et al. (2018)	Text	128	Sentences from Stanford Sentiment Treebank, Wikipedia corpus	12
Zuco 2.0	Hollenstein et al. (2019)	Text	128	Expanded subjects with similar content as Zuco 1.0	18
Envisioned Speech	Kumar et al. (2018)	Imagined Speech	14	20 text stimuli (digits, characters), 10 objects	23
Chisco	Zhang et al. (2024)	Text, Imagined Speech	128	6,681 sentences of daily Chinese expressions	3
ChineseEEG	Lu et al. (2025)	Text	128	2 Chinese novels, each character shown 350 ms without punctuation	10
Neural Spelling	Jiang et al. (2025)	Text/Handwriting	64	26 letters, tablet stylus; 25 reps/letter (650 trials)	28
OCED	Kaneshiro et al. (2015)	Image	128	12 images per 6 object categories	10
ImageNet EEG	Spampinato et al. (2017)	Image	128	40 ImageNet classes, 50 images/class, 2000 total	6
Texture Perception	Orima and Motoyoshi (2021)	Image	19	166 grayscale natural texture images	15
THINGS-EEG	Grootswagers et al. (2022)	Image	64	22,248 images across 1854 object concepts	50
DCAE	Zeng et al. (2023b)	Image	32	200 ImageNet images (cats, dogs, flowers, pandas)	26
DM-RE2I	Zeng et al. (2023a)	Image	32	200 ImageNet images across 26 subjects	26
Alljoined	Xu et al. (2024)	Image	64	10,000 images per participant from 80 MS-COCO categories	8
Low-Density EEG Reconstruction	Guenther et al. (2024)	Image	8	600 images/session (20 classes, 19 ImageNet + Faces), 2s on-screen, random shuffling	9
ThoughtViz	Tirupattur et al. (2018)	Imagined Objects	14	EEG recorded while participants imagined digits, characters, and objects	23
KARA ONE	Zhao and Rudzicz (2015)	Text, Audio, Speech	64	Rest state, stimulus, imagined speech, speaking task	12
NMED-H	Kaneshiro et al. (2016)	Music	125	4 versions of 4 songs, total 16 stimuli	48
NMED-T	Losorelli et al. (2017)	Music	128	10 songs (4:30-5:00 mins) with tempos 56-150 BPM	20
Narrative Speech	Broderick et al. (2019)	Audio	128	Audio book of <i>The old man and the sea</i> by Hemingway	19
Alice	Bhattasali et al. (2020)	Audio	61 + 1 ground	2,129 words, 84 sentences from <i>Alice in Wonderland</i>	52
N400	Toffolo et al. (2022)	Audio	128	402 sentences, each containing 5-8 words contained in <i>Medical Research Council Psycholinguistic (MRCP) database</i>	20
Japanese Speech EEG	Mizuno et al. (2024)	Audio	64	503 spoken sentences (male/female speaker)	1
Phrase/Word Speech EEG	Park et al. (2024)	Audio	64	Audio of 13 words/phrases, followed by speech replication	10

Table 1: EEG-Based Datasets from Surveyed Studies with Text, Image and Audio/Speech/Music Stimuli

occipito-parietal, and prefrontal regions and identified distinct spectral patterns associated with different colors. Green stimuli elicited **slower beta-band oscillations** over occipital areas relative to red and blue stimuli, while blue stimuli showed a **decrease in theta-band power** during the late post-stimulus period in **occipital** electrodes. The authors also reported **increased phase consistency** across trials for green stimuli, in contrast to a decrease for blue stimuli. These findings demonstrate that **color information is represented through frequency-specific and region-specific oscillatory patterns**, highlighting the potential of EEG signals to support the decoding of fine-grained visual attributes.

Collectively, these studies show that visual perception is represented in distributed, frequency-specific oscillatory patterns that evolve across cortical regions over time. This spatiotemporal structure forms the neural basis upon which EEG-to-image decoding methods can operate.

3.2. Data Acquisition

We highlight key EEG datasets captured for image stimuli in Table 1. Here, we include a key dataset to highlight relevant factors like the number and demographics of subjects, the nature of visual tasks, the image corpus, EEG recording setup, and the total size of the collected data.

Dataset experimental details: EEG-Based Visual Classification Dataset by [Spampinato et al. \(2017\)](#), has widely been used for EEG-to-image generation. The dataset was collected from **six healthy subjects** who were presented with visual stimuli drawn from a subset of ImageNet, comprising **2,000 images** (50 per class across 40 object categories). Each image was displayed for 0.5 seconds, with bursts of 25 seconds followed by a 10-second pause on a black screen. The entire experiment lasted 1,400 seconds (approximately 23 minutes). EEG was recorded using a **128-channel** actiCAP system with active, low-impedance electrodes, yielding **12,000 EEG sequences** (2,000 per subject across 6 participants). The dataset includes data al-

ready filtered in **three frequency ranges: 14-70Hz, 5-95Hz and 55-95Hz.**

This dataset has since been used in multiple studies on EEG-based image classification and visual stimulus reconstruction, making it one of the most widely used benchmarks for EEG-to-image generation studies.

3.3. Overview of Generative Models and Techniques for Image Generation

In this section, we review some key generative models and machine learning techniques for image generation as a preliminary foundation before discussing their application in the EEG-image generation domain.

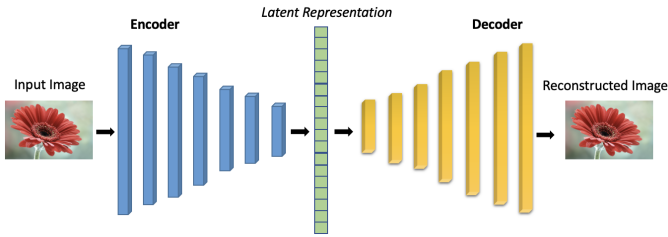


Figure 4: Traditional CNN-based encoder-decoder architecture. The encoder processes a high-dimensional input image and generates a lower-dimensional latent representation capturing the most important features of the data. The decoder then reconstructs the image from this latent representation. Model parameters are updated by minimizing the reconstruction loss between the original and reconstructed images.

A **traditional encoder-decoder architecture**, as shown in Figure 4, is a neural network framework in which the encoder takes an input and compresses it into a lower-dimensional latent representation (latent space). This concept of **dimensionality reduction** is what makes these architectures extremely useful in different domains. This process forces the model to learn the most salient and informative features (latent variables) of the input data rather than modeling every fine-grained, high-dimensional detail. The decoder then takes this latent representation and attempts to reconstruct the original input. In the context of image generation from EEG signals, this becomes a **cross-modal encoder-decoder setup**. The training data consists of EEG-image pairs, where the encoder learns to map EEG signals into a shared latent space, and the decoder learns to reconstruct the corresponding image from that representation. During training, the model **minimizes a reconstruction loss**, a measure of how different the generated image is from the original one. Minimizing this loss enables the model to **align EEG features with visual representations** in the latent space, allowing it to generate images that reflect brain signal patterns.

While encoder-decoder models are deterministic, **Variational Autoencoders (VAEs)** (Kingma et al., 2019) are probabilistic, encoding a continuous representation of the latent space. This allows them not only to reconstruct the input but also to generate new samples similar to the original data using variational inference. Instead of fixed latent variables, VAEs learn a distribution (mean and variance) over the latent variables and generate outputs by sampling from it. The latent space

should be continuous (nearby points yield similar decoded content) and complete (every point produces meaningful output). To ensure this, the latent space is regularized to follow a standard normal (Gaussian) distribution using the Kullback-Leibler (KL divergence), which minimizes the difference between the learned and target distributions. The model is trained with KL divergence loss in addition to reconstruction loss. **The probabilistic nature of VAEs might be particularly useful for EEG data, which often has a low signal-to-noise ratio.**

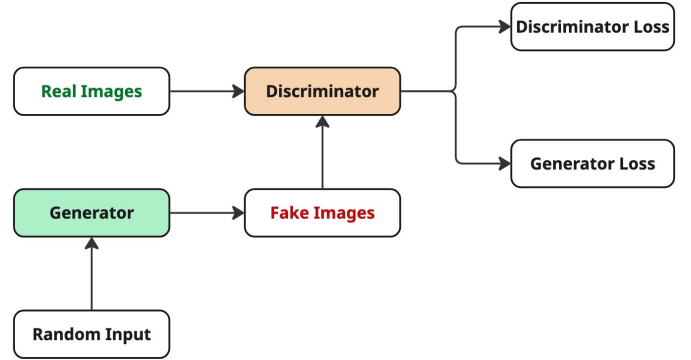


Figure 5: Structure of a Generative Adversarial Network (GAN). The model is trained through an adversarial process, where the generator creates fake images to fool the discriminator, while the discriminator learns to distinguish between real and generated images.

Another model architecture used extensively for image generation is **Generative Adversarial Network (GAN)** (Goodfellow et al., 2020), which consist of two components - a generator and a discriminator. They are trained through an **adversarial process**, where the generator produces images from random noise and attempts to fool the discriminator into classifying them as real. The discriminator, in turn, evaluates both the generated images and real samples from the training data to determine whether each is real or fake, thereby improving its ability to distinguish between them. The generator is trained using a generator loss, which measures how successfully it can deceive the discriminator; a lower generator loss indicates more realistic outputs. The discriminator loss measures how accurately the discriminator can distinguish real from fake data; a lower discriminator loss means it is effectively identifying generated samples. The outline of the adversarial process is illustrated in Figure 5. Through this adversarial training, both networks improve simultaneously, enabling the generator to produce increasingly realistic images over time.

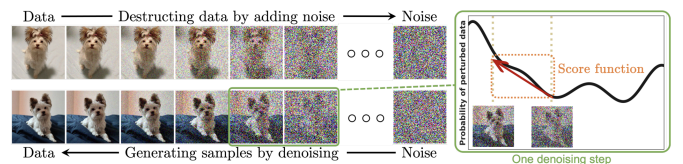


Figure 6: Probabilistic diffusion process, where data is gradually diffused into noise during the forward process, and the model learns to reconstruct data from noise by reversing these steps in the reverse diffusion process. (Yang et al., 2023b)

Diffusion models (Ho et al., 2020) are another class of generative models used for image generation. Their core idea can be understood in three stages. In the forward diffusion process, an image from the training dataset is gradually transformed into pure noise, typically following a Gaussian distribution. In the reverse diffusion process, the model learns to reverse these steps, reconstructing the original image from noisy inputs, as shown in Figure 6. During image generation, the trained model starts from random noise and progressively refines it into a high-quality image by applying the learned reverse diffusion steps. The number of steps during generation need not exactly match those used in training, since the model is trained to predict the noise added at each step rather than directly predicting the denoised image. This sampling process introduces randomness, enabling diffusion models to generate new and diverse images that closely resemble the training data. **Latent Diffusion Models (LDMs)** extend diffusion models by operating in a latent representation of the data instead of directly using high-dimensional input. This architecture employs an encoder, similar to that in a Variational Autoencoder (VAE), to first project the input image into a lower-dimensional latent space where the diffusion process is applied. The diffusion steps are thus performed more efficiently while retaining semantic quality. Stable Diffusion is a widely used implementation of this latent diffusion framework.

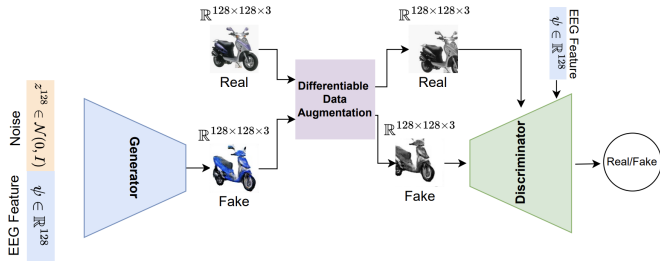


Figure 7: The Conditional GAN (cGAN) implementation from the EEG2Image framework by Singh et al. (2023) uses EEG features as conditioning inputs to guide the image generation process, enabling the model to generate images that correspond to the brain activity captured by EEG.

For **cross-modal generation**, several mechanisms such as contrastive learning, attention mechanisms, adversarial training, and conditional modeling have been employed. These approaches are often integrated with the primary generative architectures discussed above to enhance image generation from EEG signals. In the context of EEG, contrastive learning can help a model learn more robust representations by **distinguishing between EEG signals corresponding to the same image versus different images, or between signals from different subjects**. Vanilla VAEs and GANs have the limitation that users have no control over the outputs produced by the models. To generate specific or guided outputs, especially in cross-modal settings, **conditioning mechanisms** are introduced. By incorporating elements of supervised or semi-supervised learning, such as class labels or conditions, conditioning enables the model to generate outputs that are guided by specific inputs. In the context of EEG to Image generation, EEG fea-

tures are used as conditional input, as shown in Figure 7. **Well-conditioned generators** have been shown to perform better in practice (Odena et al., 2018). Conditioning can also be combined with adversarial objectives and **self-attention mechanisms** to improve image generation quality by modeling long-range dependencies (Zhang et al., 2019a) and enhancing feature consistency across modalities.

In the upcoming sections on EEG-to-image generation studies, knowledge of these fundamental generative architectures will be useful to grasp the underlying workings of proposed frameworks in this domain.

3.4. Use Cases and Addressed Concerns

Before discussing the technological aspects of generating images from EEG signals, we highlight the **key challenges addressed in existing studies**. A primary limitation lies in the **inherent noise of EEG recordings**, which results in a low signal-to-noise ratio (Bai et al., 2023; Lan et al., 2023; Zeng et al., 2023a) and restricts the amount of discriminative information that can be extracted from EEG signal. Mapping EEG embeddings and image embeddings into a shared latent space further compounds the difficulty, especially given **inter-subject variability in neural responses** (Bai et al., 2023). Cross-modal encoder-decoder networks give **limited performance on images of natural objects** compared to simpler stimuli such as digits or characters (Mishra et al., 2023) and experimental constraints often lead to **small datasets** (Singh et al., 2023), limiting the robustness and generalizability of generative models. Moreover, applying convolution layers separately along temporal and spatial dimensions has been shown to disrupt inter-channel correlations, thereby **hindering the preservation of spatial properties in brain activity** (Song et al., 2023).

To overcome the challenges of low signal quality and limited discriminative power in EEG data, Kavasidis et al. (2017), Song et al. (2023), and Mishra et al. (2023) extract **image class-specific EEG encodings** to capture features that better distinguish between categories, capture class discriminative information and therefore enhance generation quality. To overcome the loss of temporal and spatial information, Nemrodov et al. (2018) uses **spatiotemporal EEG features** to understand the neural correlates of facial identity, while Khaleghi et al. (2022) map EEG activity to **visual saliency maps** to highlight the image regions most relevant to human perception. Other approaches focus on improving alignment between brain signals and visual data: for example, projecting EEG into a shared subspace with image embeddings (Shimizu and Srinivasan, 2022) or generating **image class-specific latent representations** (Mishra et al., 2023). Similarly, Lan et al. (2023) decodes multi-level perceptual information to produce more detailed, multi-grained outputs. To overcome the large data demands of supervised learning, Li et al. (2020); Song et al. (2023) explore **alternative training paradigms** to reduce reliance on extensive labeled datasets.

Furthermore, recent studies have aimed to enhance the robustness and interpretability of EEG-based image generation. Singh et al. (2024) emphasizes on improving the **generalizability of feature-extraction pipelines** across diverse datasets

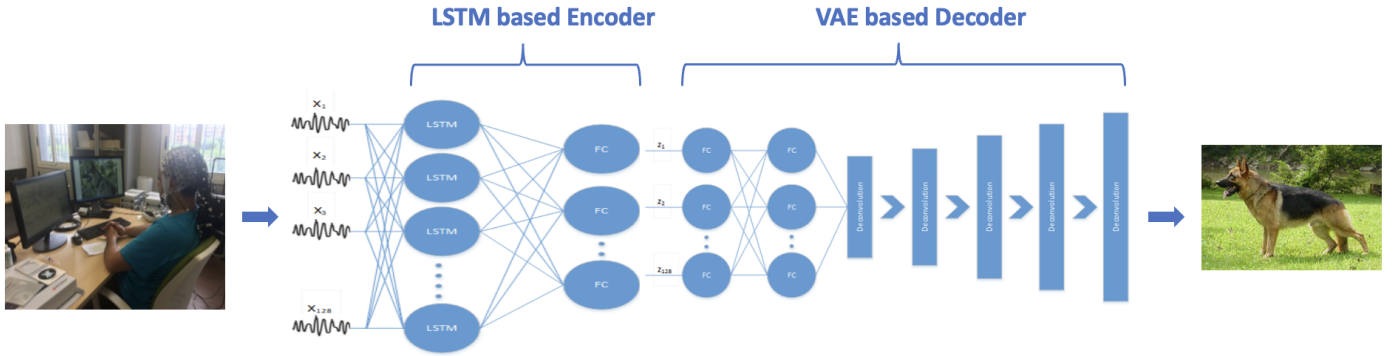


Figure 8: Encoder-decoder framework for EEG-to-image generation. In this Brain2Image implementation, an LSTM-based encoder extracts compact EEG representations, which are then mapped to the image space by a VAE-based decoder (Kavassidis et al., 2017).

, Sugimoto et al. (2024) examine the **relative contribution of different EEG electrode settings** and Li et al. (2024) explore attention mechanisms to highlight the **importance of specific channels or frequency bands**, thereby improving model performance and interpretability.

More recent studies have shifted focus toward achieving **practical BCI implementation and enhanced model interpretability**. Addressing the need for real-world usability, Guenther et al. (2024) demonstrated that image classification and reconstruction are possible using only an **8-channel portable EEG setup**, greatly improving affordability and mobility over traditional high-density systems. For a streamlined, real-time BCI, Lopez et al. (2025) proposed an **efficient pipeline** using minimal preprocessing and a lightweight adapter, successfully surpassing prior methods in both generation quality and semantic correctness.

To further prioritize interpretability and semantic fidelity, **intermediate, structured semantic representations** are used as mediators between the EEG signal and the generative model. Studies like Mehmood et al. (2025), Rezvani et al. (2025), and Cheng et al. (2025) bypass direct, noisy EEG-to-image generation by aligning EEG signals with interpretable, structured semantic prompts, such as **multilevel captions** or **fine-grained visual attributes** (e.g., color and texture). This **text-or feature-mediated approach** enables cognitively aligned decoding and precise control over the image generation process.

3.5. Generative Architectures Used Across Studies

An encoder-decoder (overview in Section 3.3) based framework, introduced in Brain2Image (Kavassidis et al., 2017), is illustrated in Figure 8 to generate images from EEG signals. Since EEG is a time-series signal with both temporal dynamics and spatial structure across electrodes, an effective **encoder must capture both dimensions**. Encoders are often designed using recurrent units (e.g., LSTMs or GRUs) to model temporal dependencies, convolutional layers to capture spatial patterns across channels, or a hybrid combination of the two. Formally, given EEG signals \mathbf{E} recorded during the presentation of a visual stimulus, the encoder f_θ maps \mathbf{E} into a latent representation $\mathbf{z} = f_\theta(\mathbf{E})$, where \mathbf{z} is compact and class-discriminative. The **decoder** then learns to generate images conditioned on

the EEG representation \mathbf{z} and is commonly implemented with CNN-based architectures such as GANs and VAEs, or more recently with Transformer and diffusion models. For further performance improvement, the **decoder can be conditioned on auxiliary information**, such as image class labels or additional EEG-derived features, which strengthens the alignment between neural representations and image space.

We provide a detailed overview of these methodologies in Section 3.3 and here we outline the major approaches found in surveyed studies, describing how they work and highlighting their relevance to the task of translating EEG signals into images specifically.

- **Variational Autoencoders (VAEs)** are well-suited for handling noisy signals and extracting structured latent features. Early work, such as Kavassidis et al. (2017); Wakita et al. (2021) employed VAEs to map EEG representations into compact embeddings that support image reconstruction tasks.
- In the context of EEG decoding, **Generative Adversarial Networks (GANs)**, have been widely used to reconstruct visual stimuli (Kavassidis et al., 2017; Khaleghi et al., 2022; Mishra et al., 2023; Singh et al., 2024; Li et al., 2024). Conditional GANs extend this by conditioning on image stimuli labels, thereby improving alignment between EEG inputs and generated outputs (Singh et al., 2023; Ahmadiieh et al., 2024).
- **Diffusion Models** are employed either to refine EEG embeddings into visual priors (Shimizu and Srinivasan, 2022) or as pre-trained backbones, such as Stable Diffusion (Bai et al., 2023). Further extensions leveraging U-Net architectures have been shown to improve reconstruction quality (Zeng et al., 2023a; Lan et al., 2023). The current state-of-the-art leverages pre-trained Latent Diffusion Models (LDMs), with recent advancements focusing on highly effective conditioning mechanisms: Guenther et al. (2024) introduced **double conditioning** to guide the LDM’s cross-attention and time-embedding simultaneously with EEG features, while Lopez et al. (2025) proposed using a **ControlNet adapter** trained exclusively on

EEG features to condition a frozen LDM, streamlining the image generation process.

- **Contrastive Learning** is used to **enhance discriminative feature extraction** (Singh et al., 2023; Lan et al., 2023; Song et al., 2023; Sugimoto et al., 2024), often using cosine similarity constraints to enforce cross-modal alignment (Song et al., 2023).
- **Attention Mechanisms** is used to weigh the relative importance of EEG channels or frequency bands, enhancing interpretability and spatial correlation modeling. They have been integrated into generative pipelines to improve both image quality and channel-level interpretability (Mishra et al., 2023; Song et al., 2023; Li et al., 2024).
- **Hybrid Strategies** adopt combined approaches to exploit complementary strengths. For example, attention modules have been integrated into GANs Mishra et al. (2023), and diffusion models have been coupled with contrastive learning frameworks Lan et al. (2023), resulting in more robust EEG-to-image generation systems. A major contemporary trend is **Semantic-Mediated Generation**, which aligns noisy EEG with an interpretable semantic space (like CLIP text embeddings or multilevel captions) that then condition a frozen Latent Diffusion Model (LDM). This semantic mediation approach is exemplified by:
 - Systems that align EEG with **CLIP text embeddings** and use **class-guided caption re-ranking** to inject context-aware information for thought visualization (Mehmood et al., 2025).
 - Models that map EEG to **multilevel captions** generated by large language models (LLMs) to enhance both the semantic alignment and the interpretability of the decoding process (Rezvani et al., 2025).
 - Frameworks that integrate both **high- and low-level semantic features** and use a conditional mechanism like FiLM (Feature-wise Linear Modulation) to achieve fine-grained control over generation (Cheng et al., 2025).

3.6. EEG Feature Encoding and Representation

Feature encoding is a critical step in EEG-to-image reconstruction, as it defines **how spatial patterns across electrodes and temporal dynamics of neural activity are extracted from raw signals** and transformed into latent representations for generation. Existing approaches can be broadly categorized into temporal modeling, spatial modeling, graph-based approaches, hybrid temporal-spatial models, and self/contrastive learning strategies.

Temporal modeling aims to analyze and learn the time-varying patterns in electroencephalogram (EEG) signals to understand brain activity over time, commonly implemented using Long Short-Term Memory (LSTM) networks, to capture temporal dependencies in EEG signals. Kavasidis et al. (2017) employ an LSTM to generate compact, class-discriminative

feature vectors that can also be used for object recognition. Building on this idea, Singh et al. (2023) integrate an LSTM encoder with a triplet-loss-based contrastive learning framework to improve feature discrimination, while Singh et al. (2024) extend the design by combining CNN and LSTM encoders under triplet-loss supervision to further enhance discriminative learning. Similarly, Ahmadih et al. (2024) apply LSTMs across EEG channels and temporal windows and augment the extracted features through regression methods, including polynomial regression, neural network regression, and fuzzy regression.

Spatial modeling uses spatial arrangement and relationships between electrode locations on the scalp to create a richer understanding of brain activity. This has been addressed primarily through **convolutional neural networks (CNNs)**, which naturally capture dependencies across EEG channels. For instance, Li et al. (2020) apply a feedforward neural network to project EEG signals into semantic features and Wakita et al. (2021) adopt a one-dimensional convolutional encoder-decoder within a multimodal VAE to get mean and variance vectors for EEG signal representation. More recent work has **integrated attention with CNN architectures**. Mishra et al. (2023) used a convolutional encoder-decoder framework enhanced with an attention module to emphasize the most informative EEG channels. Other studies leverage specialized EEG network architectures like EEGNet Lawhern et al. (2018) and Sinc-EEGNet (Bria et al., 2021), integrating attention mechanisms to highlight relevant frequency bands and channels (Sugimoto et al., 2024; Li et al., 2024).

Graph-based methods have also been explored, where EEG signals are represented as connectivity graphs. Khaleghi et al. (2022) construct graph embeddings derived from EEG functional connectivity and process them with a Geometric Deep Network (GDN) to obtain EEG feature vectors. Likewise, Song et al. (2023) integrate temporal-spatial convolution with self-attention and graph attention modules to improve feature extraction from EEG signals.

Hybrid temporal-spatial models aim to jointly exploit both domains. Zeng et al. (2023a) design a framework inspired by EEGChannelNet (Palazzo et al., 2020) and ResNet-18, combining spatial, temporal, and multi-kernel residual blocks. Similarly, Shimizu and Srinivasan (2022) introduce a **time-series-inspired architecture** with channel-wise transformations and temporal-spatial convolution to capture richer EEG representations.

Finally, **self-supervised and contrastive learning strategies** have been explored to **improve EEG feature extraction** while reducing dependence on labeled datasets. These approaches broadly fall into **two categories**: masking/reconstruction and cross-modal alignment (contrastive learning).

- Bai et al. (2023) apply **masked signal modeling** with a masked autoencoder that reconstructs partially masked EEG tokens, thereby refining latent representations.
- The **cross-modal alignment** methods primarily rely on contrastive learning to align EEG with semantic or visual

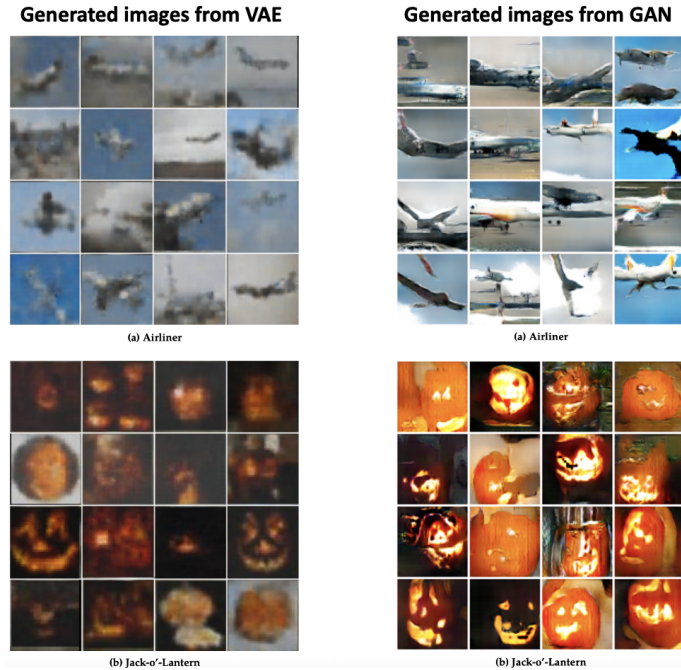


Figure 9: Examples of images generated from EEG signals for two object categories (Airplane and Jack-o’-Lantern) using VAE- and GAN-based decoders [Kavassidis et al. \(2017\)](#).

information. [Lan et al. \(2023\)](#) use contrastive learning to align EEG and image embeddings, enabling **extraction of pixel-level semantics and generation of saliency maps**; their framework further integrates **CLIP-based image caption embeddings** with an EEG sample-level encoder to strengthen cross-modal alignment. More recently, [Mehmood et al. \(2025\)](#) and [Rezvani et al. \(2025\)](#) use a symmetric InfoNCE loss (similar to CLIP) to align EEG embeddings directly with corresponding text caption embeddings.

An interesting alternative approach for semantic feature extraction is **knowledge distillation**, used by [Cheng et al. \(2025\)](#) to train a high-level EEG encoder. In this method, a frozen ResNet50 classifier provides soft-target supervision, distilling its learned representations into the EEG encoder.

3.7. Evaluation Metrics

Evaluation of EEG-to-image generation involves both **classification-based measures** (to verify that EEG features capture class discriminative information) and **image quality metrics** (to assess the fidelity and realism of generated outputs). Example of generated images from [Kavassidis et al. \(2017\)](#) are shown in Figure 9. Table 2 lists the key evaluation metrics with brief descriptions and exemplary studies that have used them.

4. EEG-to-Text Generation

4.1. Neural Basis and Signal Considerations

In this section, we highlight studies that examine EEG activity in response to text stimuli and the underlying neural basis

of language processing, which is essential for motivating how linguistic information can be reconstructed from the recorded signals.

Neural activity during reading unfolds through a sequence of cognitive operations, beginning with the **visual perception** of written text, followed by **lexical retrieval, syntactic processing**, and ultimately **semantic unification** into a coherent mental representation. Each of these stages engages distributed neural networks rather than a single brain region, and their dynamics are reflected in the **spatiotemporal oscillatory patterns** captured by EEG. Importantly, EEG frequency bands do not map one-to-one onto specific language operations; instead, language comprehension emerges from a **dynamic interplay across α , β , θ , and γ rhythms**, modulated by task demands and cortical region.

Studies show that neurocognitive aspects of language processing are associated with brain oscillations at various frequencies. A foundational review by [Bastiaansen and Hagoort \(2006\)](#) synthesizes oscillatory signatures associated with language processing. Their findings show that θ -band (4-7 Hz) synchronization increases during **memory retrieval** operations, whereas β (12-30 Hz) and γ (>30 Hz) synchronization are associated with **unification processes**, where lexical, syntactic, and semantic information are integrated.

Further evidence comes from [Bastiaansen et al. \(2008\)](#), study that investigated neural dynamics elicited by open-class (semantic-bearing) and closed-class (function) words. Both word types produced θ power increases and α/β power decreases over left occipital (visual processing) and midfrontal regions. Notably, open-class words elicited an **additional θ power increase in the left temporal cortex**, consistent with

EEG-to-Image Generation Evaluation Metrics			
Category	Metric	Description / Usage in Studies	References
Classification	Top- k Accuracy	Evaluates whether the correct class appears among the top- k predictions, confirming EEG features are class-discriminative.	Shimizu and Srinivasan (2022); Lan et al. (2023); Song et al. (2023)
Image quality / realism	Inception Score (IS)	Measures image quality and diversity using a pretrained classifier; adapted from computer vision to EEG-to-image pipelines.	Salimans et al. (2016); Kavasidis et al. (2017); Li et al. (2020); Bai et al. (2023); Singh et al. (2023)
	Frechet Inception Distance (FID)	Quantifies realism by comparing feature distributions of generated and real images.	Bai et al. (2023); Singh et al. (2024); Ahmadiéh et al. (2024)
	Kernel Inception Distance (KID)	Computes Maximum Mean Discrepancy (MMD) between real and generated distributions; complements FID.	Singh et al. (2024)
	LPIPS	Learned perceptual similarity metric that assesses patch-level similarity between generated and reference images.	Bai et al. (2023)
	Diversity Score	Diversity Score evaluates the variety of generated images, providing an indication of how well the model avoids mode collapse (i.e., producing limited or repetitive outputs).	Mishra et al. (2023)
Perceptual / Semantic	SSIM	Structural Similarity Index, measuring perceptual similarity and structural fidelity.	Khaleghi et al. (2022); Shimizu and Srinivasan (2022); Bai et al. (2023); Ahmadiéh et al. (2024); Sugimoto et al. (2024)
	PixCorr	Pixel-wise correlation coefficient between generated and target images.	Shimizu and Srinivasan (2022)
	CLIP Score	Measures semantic alignment using CLIP features against ground-truth caption or class.	Rezvani et al. (2025); Cheng et al. (2025)
	Feature Distance	Measures image similarity using features from modern backbones (e.g., AlexNet Top- k , SwAV).	Rezvani et al. (2025); Cheng et al. (2025)
Qualitative	Visual Inspection / User Study	Human-perceived quality assessment, often reported via expert visual inspection or user studies.	–

Table 2: Evaluation metrics used in EEG-to-image generation studies.

its role in lexical-semantic retrieval. Moreover, words with auditory semantic properties produced greater θ power over electrodes near the **left auditory cortex**, whereas visually descriptive words produced stronger θ responses over the left visual cortex. These findings reinforce the view that θ **synchronization supports lexical-semantic retrieval**. Studies have also linked semantic memory operations to α -band power changes.

Working memory (WM) is crucial for maintaining linguistic input during comprehension. Bastiaansen et al. (2002) associated θ synchronization with the formation of a **working-memory trace**, while Weiss et al. (2005) reported stronger θ coherence in syntactically demanding **object-relative clauses** compared to subject-relative clauses.

Semantic unification processes also demonstrate frequency-specific markers. For example, Hagoort et al. (2004) observed increased γ -band activity when sentences violated world knowledge as compared to violations of semantic features. Similarly, Weiss and Mueller (2003) found **greater γ coherence** for semantically congruent versus incongruent sentence endings.

To examine EEG coherence patterns associated with **syntactic unification**, Haarmann et al. (2002) investigated the neural processes involved in gap filling during online sentence comprehension and found that β -band coherence was significantly

larger during verb processing in sentences requiring gap filling compared to those without syntactic gaps. Extending this line of evidence, Weiss and Mueller (2012) emphasized that **β -band activity plays a key role in cognitive and linguistic manipulations during language processing**, noting its involvement in higher-order linguistic functions such as word-category discrimination, semantic memory operations, and syntactic binding that supports meaning construction during sentence comprehension.

Another important aspect of language comprehension is the **concurrent activation of multiple regions within a distributed cortical network**. Marinković (2004) showed that processing written words begins in sensory-specific occipital areas and then progresses anteriorly along the ventral processing streams toward supramodal regions, including the temporal and inferior prefrontal cortices. The integration of a word into its contextual meaning peaks around **400 ms after word onset**, driven largely by coordinated activity between left temporal and inferior prefrontal regions during reading. EEG studies further support this spatiotemporal progression: Fahimi Hnazaee et al. (2018) reported that early word processing starts with visual processing in the occipital cortex, followed by activation along the ventral stream—first engaging left posterior occipital regions around **200 ms**, then reaching the posterior temporal

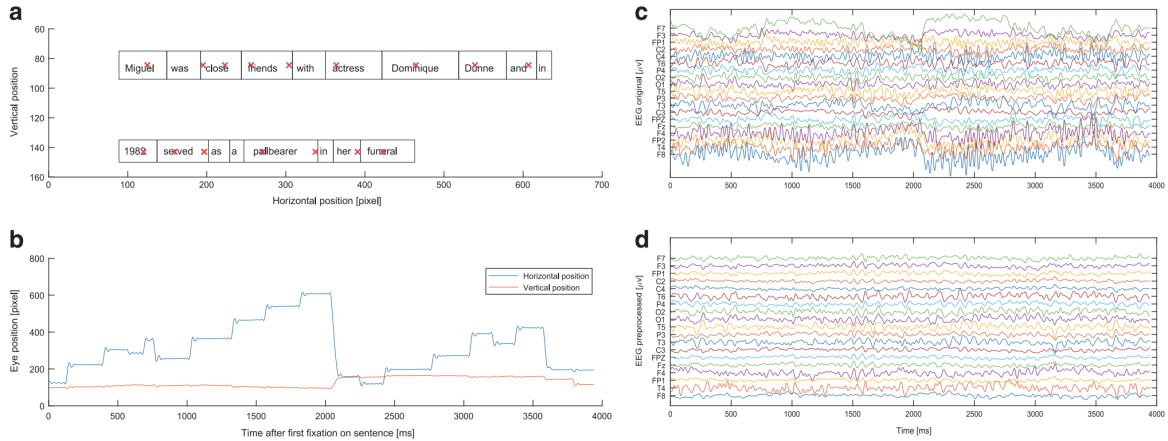


Figure 10: Visualization of single trial EEG and eye-tracking data (Hollenstein et al., 2018) (a) Fixations at the word level EEG marked with red cross and boxes. (b) Raw fixation gaze data. (c) Raw EEG signals. (d) EEG signals after preprocessing.

cortex during the **semantic-processing window (around 400 ms)**. At later stages, anterior temporal, inferior frontal, and orbital regions become involved, reflecting the transition from perceptual processing to higher-order lexico-semantic integration.

Together, these findings demonstrate that EEG captures a rich hierarchy of lexical, syntactic, and semantic processes distributed across cortical networks, providing the neural foundation from which EEG-to-text generation models attempt to decode and reconstruct linguistic information.

4.2. Data Acquisition

We highlight major EEG datasets captured for text stimuli in Table 1. For such datasets, the most relevant factors are the number and demographics of subjects, the nature of tasks performed, the EEG recording setup, the method of aligning neural signals with text (often via eye-tracking), and the overall dataset size.

ZuCo Dataset experimental details: To provide additional context, we describe the data acquisition process for **one key dataset**, the Zurich Cognitive Language Processing Corpus (ZuCo) (Hollenstein et al., 2018), which has become a benchmark for EEG-text research. The dataset was collected from **12 healthy native English speakers** engaged in naturalistic reading tasks, where **sentences were drawn from the Stanford Sentiment Treebank** (movie reviews) **and the Wikipedia Relation Extraction corpus** (famous people labeled with relation types). Participants completed **three tasks**: sentiment analysis of movie reviews, relation recognition in Wikipedia sentences, and a task-specific relation classification, with a total reading duration of 4-6 hours per subject across two sessions.

Eye movements were simultaneously recorded with an Eye-Link 1000 Plus tracker (sampling rate of 500 Hz). Eye movement data is essential for providing word-level alignment between text and EEG signals, as it defines the precise onset and duration of fixations during reading. Figure 10 shows how eye position coordinates are used to capture word boundaries. High-density EEG was captured using a **128-channel Hydro-**

Cel system (500 Hz, 0.1-100 Hz bandpass). The final corpus includes over 21,000 words across 1,100 sentences and approximately 154,000 gaze fixations, providing a uniquely synchronized dataset of EEG and eye-tracking signals.

ZuCo Dataset frequency bands: EEG signals captured across entire task period for **eight different frequency bands** resulting in a time-series for each frequency band - θ_1 (4-6 Hz), θ_2 (6.5-8 Hz), α_1 (8.5-10 Hz), α_2 (10.5-13 Hz), β_1 (13.5-18 Hz), β_2 (18.5-30Hz), γ_1 (30.5-40 Hz), γ_2 (40-49.5 Hz).

Word level EEG Input for ZuCo: Out of 128 channels, 9 EOG channels were used for artifact removal. Additionally, 14 channels primarily located on the neck and face were excluded from analysis. **Each word-level EEG feature has a fixed dimension of 105.** To obtain word level EEG input, EEG data was aggregated on gaze duration. Features are concatenated from all 8 frequency bands, into one **feature vector with a dimension of 840.**

By enabling precise mapping between neural activity at word-level, ZuCo supports applications in NLP tasks such as sentiment analysis and relation extraction, as well as cognitive neuroscience research on natural reading. Beyond reading and comprehension analysis, the ZuCo dataset has also been used extensively in EEG-text generation studies.

4.3. Overview of Generative Models and Techniques for Text Generation

In the domain of text generation, technological advancements are largely driven by probabilistic language models. Early foundational work dates to the early 2000s, when **Bengio et al. (2003)** proposed "*learning a statistical model of the distribution of word sequences by neural networks*", such that word representations capture the probability distribution of natural language sequences. Given a context c (a set of preceding words), the **model predicts the next word w in the sequence according to the conditional probability $P(w | c)$** , where $|c|$ denotes the size of the context window. This core **autoregressive principle** extends naturally to **Large Language Models (LLMs)**, which are trained on vast amount of data and can be

trained or fine-tuned to perform tasks in diverse domains, from text-to-text generation (prompt-based) to **cross-modal generation** such as image-to-text, audio-to-text, or even EEG-to-text translation.

The text generation models inherently perform temporal modeling i.e. predicting the next element in a sequence, which aligns closely with the temporal dynamics of EEG signals. Moreover, their ability to support many-to-many sequence generation (as in machine translation tasks) makes them particularly suitable for EEG-to-text generation applications. For EEG-to-text generation, we provide an overview of **language models** that are either used to **obtain robust EEG representations** for text generation (such as RNNs and GRUs) or that **utilize EEG representations to generate natural language text** (such as large language models (LLMs) like BART).

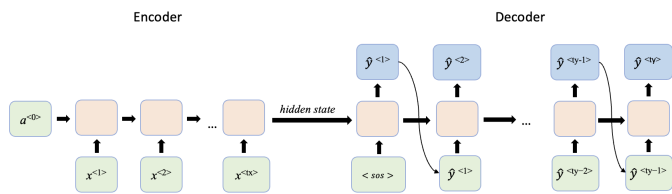


Figure 11: A traditional RNN architecture for many-to-many sequence generation in a machine translation task. It consists of an **encoder** that processes the input sequence x and a **decoder** that takes the encoder's hidden state a as input and autoregressively generates the output sequence \hat{y} . The diagram shows an unrolled RNN illustrating sequence processing at each time steps t .

Recurrent Neural Networks (RNNs), in contrast to simple feedforward neural networks, allow previous outputs to be reused as inputs through hidden states, enabling them to **model sequential dependencies in time-series data**. Given a sequence $x_1, x_2, x_4, \dots, x_{t-1}, x_t$, the activation corresponding to x_1 is used in processing x_2 , and so on, as illustrated in Figure 11. This recurrent structure allows RNNs to **"remember" previous information and maintain context over time**, which is particularly useful for capturing temporal dependencies in data such as EEG signals and natural language. However, as information propagates over many time steps, RNNs struggle to capture long-term dependencies due to the vanishing and exploding gradient problems. To overcome these limitations, advanced variants such as **Long Short-Term Memory (LSTM)** and **Gated Recurrent Unit (GRU)** networks have been proposed. **LSTMs** introduce memory "cells" in the hidden state, regulated by three gates: the forget gate (determining what information to discard), the input gate (selecting what new information to store), and the output gate (controlling what information is passed to the next time step). **GRUs**, on the other hand, simplify this mechanism by using only two gates: reset and update, and by merging the cell and hidden states, thus **reducing computational complexity while maintaining comparable performance**. Additionally, Bidirectional RNNs (BiRNNs) extend these architectures by processing the sequence in both forward and backward directions, allowing the model to incorporate context from both past and future time steps. In the context of EEG-to-text generation, RNN-based architectures, including LSTMs, GRUs, and BiRNNs, are frequently employed

for EEG feature extraction due to their ability to effectively capture the temporal dynamics inherent in EEG signals.

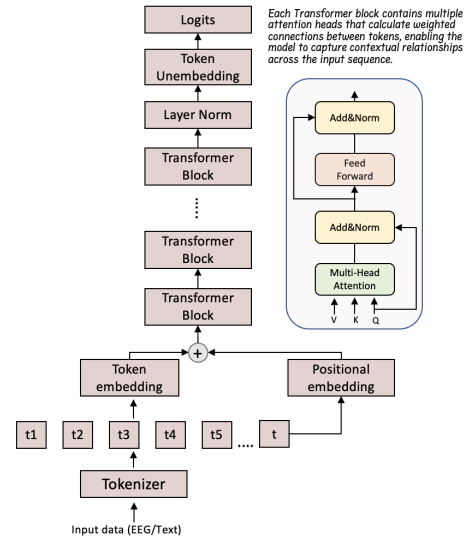


Figure 12: Multi-layer Transformer architecture and Transformer block illustration. The model takes a sequence as input and outputs logits, which are then used to generate text.

Over the past decade, **Transformer architectures** have dominated text generation, particularly in sequence-to-sequence (seq2seq) applications. While RNNs process data sequentially at each time step, they are limited in their ability to capture long-range dependencies within the data. **Transformers, with their self-attention mechanism, can model multiple dependencies simultaneously**. In a traditional Transformer based architecture, as shown in Figure 12, the input data is first divided into tokens, which are then passed to a series of transformer layers where the **attention mechanism** assigns weights that represent the relationships between these tokens, allowing the model to "attend" to the most relevant parts of the input sequence. This mechanism, combined with the Transformer's ability to process data in parallel, greatly enhances its capacity to capture complex relationships and dependencies in large-scale datasets.

A **typical EEG-to-text generation framework**, illustrated in Figure 13, consists of a **multi-layer Transformer**, used as a **pre-encoder** to extract embedding representations from EEG signals. These embeddings are then passed to a **pre-trained BART** (Bidirectional and Auto-Regressive Transformer) language model **to generate text from EEG-derived features**. **BART** employs a bidirectional encoder that captures contextual information in both directions to learn latent EEG representations, and an autoregressive decoder that generates coherent natural language text based on these learned representations.

In addition to this, for cross-modal learning, techniques such as **contrastive learning and masked signal modeling** have been employed. **Contrastive learning**, as described in Section 3.3, helps the model learn more robust representations by distinguishing between EEG signals corresponding to the same text versus different text, or between signals from different subjects in EEG-to-text generation. In **masked signal modeling**,

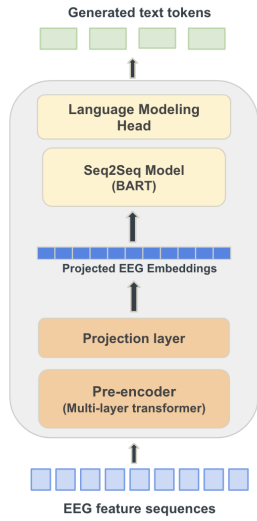


Figure 13: Illustration of the EEG-to-Text framework adapted from Wang and Ji (2022). The framework employs a multi-layer Transformer to extract EEG embeddings from input features, followed by an encoder-decoder based BART language model that generates text from the projected EEG embeddings.

portions of the input sequence are masked, and the encoder is trained to reconstruct the original sequence, thereby learning **robust contextual representations**. Separate Transformer-based encoders, such as BART or other multi-layer Transformers, have been used independently for text and EEG masked signal modeling.

This overview provides a strong foundation for the upcoming sections, where we discuss how they have been integrated into various architectures for EEG-to-text generation tasks.

4.4. Use Cases and Addressed Concerns

In the domain of generating text from EEG signals, early work has typically relied on **closed-vocabulary approaches**, where decoding is limited to a fixed set of predefined words (Biswal et al., 2019; Srivastava and Shinde, 2020; Yang et al., 2023a; Rathod et al., 2024). Among these, Srivastava and Shinde (2020) and Yang et al. (2023a) explore the use of Morse code representations, in which users’ active intent is mapped to Morse sequences that are subsequently translated into text.

More recent studies have moved toward **open-vocabulary generation**, enabling decoding beyond fixed word sets and aiming to support naturalistic conversation (Wang and Ji, 2022; Feng et al., 2023; Duan et al., 2023; Liu et al., 2024a; Wang et al., 2024; Amrani et al., 2024; Tao et al., 2024; Mishra et al., 2024; Ikegawa et al., 2024; Chen et al., 2025; Gedawy et al., 2025; Masry et al., 2025; Liu et al., 2025; Lu et al., 2025; Jiang et al., 2025). These works address several important concerns, including **subject-dependent variability** in EEG representations (Feng et al., 2023; Amrani et al., 2024; Gedawy et al., 2025), learning **cross-modal alignment** between EEG and text embeddings (Wang et al., 2024; Tao et al., 2024), and **modeling long-term dependencies and contextual information** that may be missed by conventional architectures (Rathod et al., 2024; Chen et al., 2025).

A persistent challenge in EEG-to-text research is the **reliance on eye-tracking fixation data** to define word-level markers, which has been addressed by studies such as Duan et al. (2023) and Liu et al. (2024a). To mitigate the difficulty of defining word boundaries in EEG signals and to **broaden applicability across languages**, some studies have proposed **language-agnostic solutions** (Mishra et al., 2024; Ikegawa et al., 2024), where signals are captured through visual stimuli and decoded via advances in image-text intermodality. **Data scarcity** also remains a limiting factor, and Yu-Hao Chen et al. (2025) propose a VAE-based augmentation technique to expand EEG-text datasets and improve training efficiency.

Another major concern has been the semantic fidelity of generated text, since shallow lexical matching often fails to capture the intended meaning of the text. Approaches that explicitly encourage interpretable and semantically aligned representations, for example through contrastive learning (Feng et al., 2023; Tao et al., 2024; Liu et al., 2025), have been introduced to **reduce semantic drift and improve the quality of open-vocabulary generation**. Relatedly, **cross-lingual generalization** has begun to receive attention, with studies like Lu et al. (2025) demonstrating that EEG-to-text decoding can extend beyond English by aligning Chinese EEG signals with text embeddings.

Beyond reading-based tasks, EEG signals associated with handwriting have been used to decode individual alphabet letters to further generate fluent text, aiming toward a Spell-Based BCI System (Jiang et al., 2025).

4.5. Generative Architectures Used Across Studies

EEG-to-text generation draws on a diverse set of modeling and representation learning approaches. We have found that **sequence-to-sequence (seq2seq) generation** serves as a major overarching framework. The idea is to formulate EEG to text generation as a **neural machine translation task** (Wang and Ji, 2022) and maximizing the probability of decoded sentence which is the conditional probability of predicting the sequence s_t , given the EEG signal \mathcal{E} and previously decoded sequences, where T is the length of the target text sequence:

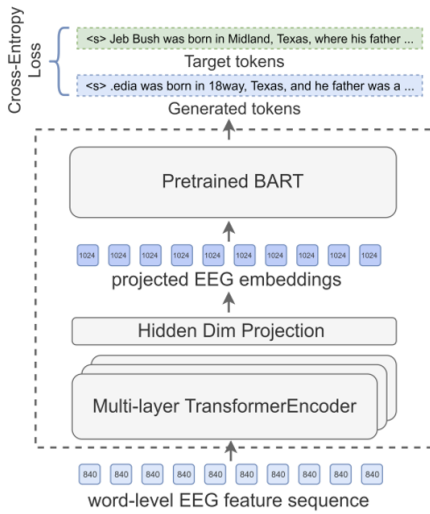
$$p(\mathcal{S}|\mathcal{E}) = \prod_{t=1}^T p(s_t \in \mathcal{V}|\mathcal{E}, s_{<t}) \quad (1)$$

After extracting word-level EEG inputs, as described in Section 4.2, an EEG-to-text decoding framework similar to Figure 14 is used to generate output text. Instead of requiring an exact sentence-level match, the generated text is evaluated against the original reference using semantic similarity and word-overlap metrics.

We now outline the major state-of-the-art techniques applied to EEG-to-text generation, explaining the underlying approach of each method and its relevance.

- **Large Language Models (LLMs)** are widely used due to their ability to capture **long-range dependencies in text** and generate coherent linguistic output. Several studies employ BART as the core text generation model (Wang

a. EEG to Text decoding framework



b. Ground Truth vs Decoded Sentences examples

(1)	Ground Truth: He is a prominent member of the Bush family , the younger brother of President George W. Bush ...
	Model Output: was a former member of the American family , and son brother of President George W. Bush ...
(2)	Ground Truth: Raymond Arrieta (born March 26, 1965 in San Juan, Puerto Rico) is considered by many to be one of Puerto Rico's greatest comedians .
	Model Output: mond wasaga ,19 in 17, 18) New Francisco, Puerto Rico) is a one many to be the of the Rico's greatest poets .
(3)	Ground Truth: He was first <i>appointed</i> to fill the Senate seat of Ernest Lundeen who had died in office.
	Model Output: was a <i>elected</i> to the the position seat in the Hemy in died died in 18 in
(4)	Ground Truth: Adolf Otto Reinhold Windaus (December 25, 1876 - June 9, 1959) was a significant <i>German chemist</i> .
	Model Output: rian Hitler ,hard,eren18 18, 1885 - January 3, 18) was a <i>German figure-</i> and
(5)	Ground Truth: It's <i>not a particularly good</i> film, but neither is it a <i>monstrous</i> one.
	Model Output: was a a <i>bad good</i> story, but it is it <i>bad bad</i> . one.

Figure 14: (a) EEG decoding framework that takes word level EEG as input and follows a sequence-to-sequence neural machine translation task to predict output text. (b) Comparison of Ground Truth and Decoded sentences for exact word match and semantic resemblance (Wang and Ji, 2022).

and Ji, 2022; Liu et al., 2024a; Wang et al., 2024; Amrani et al., 2024; Tao et al., 2024; Chen et al., 2025). In addition, Mishra et al. (2024) fine-tuned LLMs on EEG embeddings alongside image-text data during training, enabling text generation directly from EEG signals during inference. Liu et al. (2025) introduces a contrastive-generative framework that aligns EEG representations with a frozen Flan-T5 (LLM) latent space, (Jiang et al., 2025) explores letter-level decoding followed by generation with BART language model.

- **Contrastive learning** is frequently applied to align EEG and text embeddings in a shared space, further **enhancing cross-modal alignment and improve feature discrimination** (Feng et al., 2023; Tao et al., 2024; Wang et al., 2024; Liu et al., 2025).
- **Masked signal modeling** is used as **self-supervised pre-training strategy** to learn robust EEG representations. For example, Liu et al. (2024a) employ a transformer trained to reconstruct randomly masked segments of EEG data, thereby learning contextual and semantic dependencies at the sentence level. An integrated framework by Tao et al. (2024) combines contrastive learning with masked signal modeling, where word-level EEG feature sequences are randomly masked and sentence-level sequences deliberately masked, guided by an **intra-modality self-reconstruction objective**.
- **Recurrent Neural Networks (RNNs)** have been adopted to capture the sequential dynamics of EEG signals. Amrani et al. (2024) use bidirectional GRUs to process word-level EEG signals of varying lengths, while Chen et al. (2025) extend this to a **hierarchical GRU** design that **captures both local contextual information and long-range dependencies** through the organization of hidden layers

hierarchically. Similarly, Gedawy et al. (2025) employs bidirectional GRUs to model temporal dynamics followed by a subject-specific adaptation layer to extract subject-dependent features.

- **Ensemble-based methods** have also been explored to enhance robustness and address class imbalance in the dataset. Rathod et al. (2024) propose a folded ensemble deep CNN for text suggestion and a folded ensemble bidirectional LSTM for text generation, to improve accuracy of generated text.

4.6. EEG Feature Encoding and Representation

Feature encoding is a critical step in EEG-to-text generation, as it transforms raw neural activity into structured representations aligned with linguistic output. Several distinct approaches have been proposed for encoding EEG signals, varying in how they model temporal dynamics, spatial dependencies, and higher-level semantic representations.

Spatial-Temporal EEG Features are critical for effective EEG-to-text decoding. Biswal et al. (2019) extract **shift-invariant features** using stacked CNNs and model **temporal dependencies** using RCNNs, followed by processing by hierarchical LSTMs for medical report generation. Similarly, Srivastava and Shinde (2020) combine spatial variation modeling using CNNs with extracting temporal dynamics with LSTMs, while Yu-Hao Chen et al. (2025) enhance feature extraction under both classification and seq2seq objectives by incorporating **residual blocks to effectively capturing spatial-temporal EEG patterns**. This strategy continues in recent work, where to better represent **spatial feature maps and temporal dependencies across subjects**, bi-GRUs paired with subject-adaptive encoders and transformer layers are employed Gedawy et al. (2025). More recently, Alharbi and Alotaibi (2024) propose

EEG-to-Text Generation Evaluation Metrics			
Category	Metric	Description / Usage in Studies	References
Lexical overlap	BLEU	n -gram precision overlap between generated and reference text.	Papineni et al. (2002); Biswal et al. (2019); Wang and Ji (2022); Feng et al. (2023); Mishra et al. (2024); Gedawy et al. (2025); Masry et al. (2025); Liu et al. (2025); Lu et al. (2025); Jiang et al. (2025)
	ROUGE	Recall-oriented lexical overlap, emphasizes n -gram recall.	Lin (2004); Wang and Ji (2022); Feng et al. (2023); Duan et al. (2023); Liu et al. (2024a); Wang et al. (2024); Mishra et al. (2024); Gedawy et al. (2025); Masry et al. (2025); Liu et al. (2025); Lu et al. (2025)
	METEOR	Includes stemming and synonymy for nuanced alignment.	Banerjee and Lavie (2005); Biswal et al. (2019); Chen et al. (2025); Mishra et al. (2024); Masry et al. (2025); Gedawy et al. (2025)
Semantic similarity	BERTScore	Embedding-based contextual similarity beyond lexical overlap.	Zhang et al. (2019b); Amrani et al. (2024); Mishra et al. (2024); Gedawy et al. (2025); Liu et al. (2025)
	BLEURT	Learned evaluation metric based on pretrained language models.	Sellam et al. (2020); Chen et al. (2025)
Error-based	WER	Word-level transcription error rate.	Feng et al. (2023); Jiang et al. (2025)
	TER	Translation Error Rate; number of edits required to match reference.	Chen et al. (2025)

Table 3: Evaluation metrics used in EEG-to-text generation studies.

a hybrid deep learning model that combines 3D CNNs with various RNN architectures (LSTM, stacked LSTM, BiLSTM) to jointly capture spatial and temporal dynamics in EEG for speech decoding.

Spectral and Statistical Features are incorporated in some studies to enrich EEG representations beyond spatio-temporal patterns. Spectral features capture the distribution of signal energy across frequency bands, such as power spectral density, band power, or spectral entropy, providing information about oscillatory brain activity. Yang et al. (2023a) apply the **Short-Term Fourier Transform (STFT) to derive these spectral features** and concatenate them with **statistical measures** (e.g., minimum and maximum per channel), combining them with CNNs and RNNs to model spatial and temporal dynamics, respectively. Similarly, Rathod et al. (2024) employ **Wavelet Transform (WT), Common Spatial Patterns (CSP), and statistical descriptors** to construct discriminative feature vectors for closed-vocabulary text classification. For open-vocabulary decoding, Masry et al. (2025) use a combination of EEG spectral features and **synchronized eye-tracking features**: fixation duration (FFD), total reading time (TRT), and gaze duration (GD) to drive joint generation and sentiment classification.

Contextual EEG Representations have recently been advanced through transformer-based architectures that excel at modeling long-range dependencies. Wang and Ji (2022) employ a multi-layer transformer encoder to map word-level EEG sequences into text representations, while Feng et al. (2023) use a transformer-based pre-encoder to **project word-level EEG features into the Seq2Seq embedding space**. Building on this, Tao et al. (2024) introduce a **cross-modal codebook that stores EEG embeddings alongside word embeddings** obtained from BART. To further enhance **contextual EEG representations** neural signals are aligned with pre-trained language

model spaces. In this paradigm, Liu et al. (2025) aligns neural features with a frozen Flan-T5 latent space, enabling semantically grounded and interpretable EEG-to-text decoding, while Lu et al. (2025) align transformer-based EEG decoding with MiniLM embeddings to improve cross-modal contextual decoding.

Marker-Free and Sentence-Level EEG Representations address the limitations of relying on eye-tracking markers, which restrict the generalizability of word-level EEG features. Duan et al. (2023) extract both marker-aligned word-level features using multi-head transformers and raw EEG embeddings without markers using a multi-layer transformer encoder. For raw EEG waves, the encoder is trained to self-reconstruct waveforms while transforming signals into sequences of embeddings. Liu et al. (2024a) pretrain a convolutional transformer on sentence-level EEG signals with a masking objective and employ a multi-view transformer to separately encode brain regions using dedicated convolutional transformers. Similarly, Wang et al. (2024) integrate word-level and sentence-level EEG features, applying random masking at the word level and compulsory masking at the sentence level to enhance contextual representations.

Hierarchical Temporal EEG Representations continue to be effectively modeled using recurrent-hierarchical architectures. Chen et al. (2025) propose a hierarchical GRU decoder with a Masked Residual Attention Mechanism to capture both **local and global contextual information**. Similarly, Amrani et al. (2024) employ bidirectional GRUs to process **variable-length word-level EEG sequences**, integrating them with a subject-specific 1D convolutional layer and a multi-layer transformer for richer feature encoding.

More recently, **Topographic maps** have been used by Alharbi and Alotaibi (2024) to capture the **brain’s dynamic re-**

sponses, where raw EEG for each 'imagined word' is represented as a single image composed of sixteen time-domain topographic brain maps, to capture both spatial distributions across electrodes and temporal dynamics of EEG into a unified representation.

4.7. Evaluation Metrics

Evaluation of EEG-to-text generation relies on established natural language processing metrics that compare generated text against reference text. As noted previously, the generated text is compared with the original reference using semantic similarity and word-overlap measures, rather than requiring an exact sentence level match. Figure 14 (b) shows example of actual and decoded sentences. The metrics can broadly be grouped into **lexical overlap metrics, semantic similarity metrics, and error-based metrics**. Table 3 lists the key evaluation metrics with brief descriptions and exemplary studies that have used them.

5. EEG-to-Audio/Speech Generation

5.1. Neural Basis and Signal Considerations

Different types of sound stimuli, such as **pure tones, speech, and music**, elicit distinct patterns of brain activity across cortical regions. When captured through EEG, this activity is reflected in the amplitudes or spectral power of different EEG frequency bands which vary across brain regions and reveal how auditory information is processed in the brain. Primarily, **sound is identified and processed in the auditory cortex located within the temporal lobe**, however, auditory processing is not confined to this region alone. Several studies have examined how the brain responds to different types of auditory stimuli.

As observed by Krause et al. (1997), neural signals evoked by sound stimuli that do not involve higher-level processing such as semantic interpretation or memorization are likely processed primarily within the auditory cortex, which is part of the temporal lobe. In contrast, **sound stimuli requiring speech perception engage additional brain regions beyond the auditory cortex**. To evaluate this distinction, the authors compared EEG responses while subjects listened to text played backward (lacking high-level processing) and text played forward (involving semantic comprehension).

For both types of stimuli, synchronization and desynchronization of EEG α band activity (8-10 Hz and 10-12 Hz) were observed. Generally, increased cortical activity is associated with a decrease in α amplitude, meaning that α desynchronization signifies cortical activation. In the 10-12 Hz band, listening to forward (meaningful) text elicited desynchronization, whereas listening to backward (non-semantic) text elicited synchronization in the parieto-occipital area. The increased activity (synchronization) observed in the parieto-occipital area while listening to backward text indicates that **auditory stimuli not involving higher level processing (semantics or memorization) are processed directly on the auditory cortex**. This dissociation was not observed in the 8-10 Hz band, where

both stimulus types produced event-related desynchronization (ERD), which the authors attributed to non-specific cognitive processes such as sustained attention.

However, some studies examining the characteristics of different brain waves across brain regions have reported frequency-specific activity in multiple cortical areas, even for sound stimuli that do not require higher-level processing. Di et al. (2018) investigated EEG responses to intermittent pure tone stimuli, analyzing θ (4-7.5 Hz), α (8-13 Hz), and β (14-30 Hz) waves across different brain regions, specifically, the four lobes (frontal, temporal, parietal, occipital) and both hemispheres (eight regions in total). The study found that **mean theta-wave amplitudes** differed significantly among the frontal, temporal, and parietal regions (but not the occipital region) across four time periods, one with sound stimulation and three without, highlighting the **significance of temporal factors on auditory EEG responses**. Significant interaction effects were also observed for **mean alpha wave amplitude** in the frontal region, and a significant main effect of hemisphere was found in the temporal region. Additionally, differences in the interaction among hemisphere, frequency, and loudness were detected in the mean beta-wave amplitude within the parietal region, suggesting that **auditory processing of even simple tone stimuli involves complex, region and frequency dependent neural dynamics**.

Other studies, such as Farahani et al. (2021), have examined both cortical and subcortical contributions to auditory processing in the brain. **Relatively high sound modulation frequencies (e.g., 40 and 80 Hz) are believed to engage subcortical neural generators more strongly than cortical ones** (Herdman et al., 2002). To investigate these mechanisms, researchers often analyze Auditory Steady-State Responses (ASSRs), which are brain responses evoked by modulated or repetitive acoustic stimuli and serve as reliable indicators of auditory temporal processing. Because of its excellent temporal resolution, EEG is particularly well-suited for capturing the auditory system's synchronized responses to such stimuli, providing rich information about the dynamics of neural activity and the interaction between cortical and subcortical brain networks involved in auditory perception.

These findings form the neurophysiological basis for EEG-to-audio generation. The observed synchronization and desynchronization patterns, frequency-specific activations, and cortical-subcortical interactions reflect how the brain encodes different aspects of auditory information. **EEG signals thus capture both low-level acoustic features and higher-level speech perception**. EEG-to-audio techniques aim to leverage these patterns to reconstruct or generate audio by learning the mapping between neural activity and auditory representations.

5.2. Data Acquisition

We summarize major EEG datasets collected for audio-related stimuli in Table 1. For speech-synthesis tasks, datasets may be recorded using either audio or text prompts, with participants engaged in reading, vocalized speech, or imagined speech activities. We highlight a representative dataset to il-

illustrate how EEG data are collected, including details on the recording equipment and experimental stimuli and tasks.

Dataset Experimental Details: A notable resource for EEG-to-speech synthesis is the **KARA ONE corpus** (Zhao and Rudzicz, 2015), which includes recordings of both **imagined and vocalized speech**. This multimodal dataset integrates **EEG, facial motion, and audio** data. Recordings were collected from **12 participants** using a **64-channel Neuroscan Quick-Cap** for EEG acquisition and a **Microsoft Kinect (v1.8)** sensor to capture synchronized facial video and speech audio.

Each recording session lasted approximately **30–40 minutes** and consisted of repeated sequences of four successive states: (i) a 5-second rest state, (ii) a stimulus state in which a text prompt appeared on screen and its auditory utterance was played through speakers, followed by a 2-second preparation phase (iii) a 5-second **imagined speech** state, and (iv) an overt **speaking state**, in which participants vocalized the prompt while facial and audio data were captured by the Kinect.

In total, each prompt was presented **12 times** across **132 trials**. The stimuli included **seven phonemic/syllabic prompts** (/iy/, /uw/, /piy/, /tiy/, /diy/, /m/, /n/) and **four phonetically similar words** (*pat, pot, knew, gnaw*), selected to balance nasals, plosives, and vowels, as well as voiced and unvoiced phonemes. The data was filtered between 1 and 50 Hz, and mean values were subtracted from each channel. This multimodal dataset provides a valuable benchmark for studying both imagined and spoken speech decoding from EEG.

5.3. Overview of Generative Models and Techniques for Audio Generation

In this section, we provide an overview of the machine learning models and techniques used for EEG-to-audio generation. Some of the underlying architectures, such as RNNs, GRUs, Transformers, and Latent Diffusion Models, have already been discussed in Section 3.3 and Section 4.3. Readers are referred to these sections for an overview of their architectures and functionality.

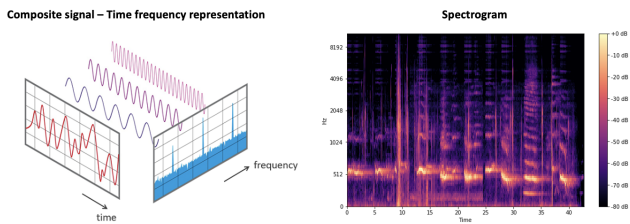


Figure 15: Time-frequency representation of a composite signal and a spectrogram representation showing time on the x-axis, frequency on the y-axis, and color intensity indicating signal amplitude.

Signal-based data, contains both frequency and time-domain components, is illustrated in Figure 15. Instead of a single frequency, the actual signal is a composite waveform formed by the superposition of multiple frequencies. In the context of EEG, **band-pass filtering** is applied to separate specific frequency bands from the raw composite EEG

data. When applying deep learning techniques, instead of using raw signal data directly, it is often transformed into an image representation. These image representations are typically mel-spectrograms. Of the surveyed studies in the domain of EEG-to-Audio/Speech generation, **most studies use mel-spectrogram as the intermediate input**.

A spectrogram, shown in Figure 15, is a **visual representation of a signal with time on the x-axis and frequency on the y-axis**, providing a snapshot of how the frequency content of a composite waveform evolves over time. It uses color intensity to indicate the amplitude or power of each frequency component. Spectrograms are created using Fourier Transform, which decompose the signal into its constituent frequencies and displays the amplitude of each frequency present in the signal. In the case of audio signals, a mel-spectrogram is used, which applies the mel scale (a nonlinear, logarithmic frequency scale based on human auditory perception) on the y-axis and represents amplitude in decibels through color. **Mel-spectrograms more closely reflect human perception of audio and music**. For EEG-to-audio generation, to maintain representation consistency between modalities, several studies used mel-spectrograms for both EEG and audio data.

Deep learning models such as **Convolutional Neural Networks (CNNs)**, **Recurrent Neural Networks (RNNs)**, and hybrid architectures like **CNN-GRU** can be employed to generate spectrograms. In the EEG-to-audio generation domain, these models are trained to **construct spectrograms from EEG signals by minimizing the loss between EEG-generated and audio-generated spectrograms**, as shown in Figure 16. **Neural vocoders** such as the High-Fidelity Generative Adversarial Network (HiFi-GAN) (Kong et al., 2020) are then used to reconstruct audio waveforms using the learned spectrogram representations. **HiFi-GAN**, in addition to being a GAN-based architecture, employs two types of discriminators: **multi-scale discriminators**, which analyze the generated audio at different scales or resolutions, and **multi-period discriminators**, which learn diverse implicit structures by examining different parts of the input. This combination allows HiFi-GAN to **capture both the overall speech structure and fine-grained details**, thereby producing longer, high-fidelity audio outputs.

An overview of composite signals, mel-spectrogram representations, and the model architectures discussed in this and previous sections for image and text generation provides a strong foundation for the upcoming sections, where we examine how these models have been integrated into various architectures for EEG-to-audio/speech generation tasks.

5.4. Use Cases and Addressed Concerns

For EEG-based audio/speech generation, reported use cases include **speech synthesis** (Krishna et al., 2021; Lee et al., 2023a), **music decoding and reconstruction** (Ramirez-Aristizabal and Kello, 2022; Postolache et al., 2024), **emotive music generation** (Jiang et al., 2024), **voice reconstruction** (Lee et al., 2023b), **talking-face generation** Park et al. (2024), and **speech recovery** (Mizuno et al., 2024). While many of these studies focus on decoding auditory information during listening tasks in speech or music perception (Krishna et al.,

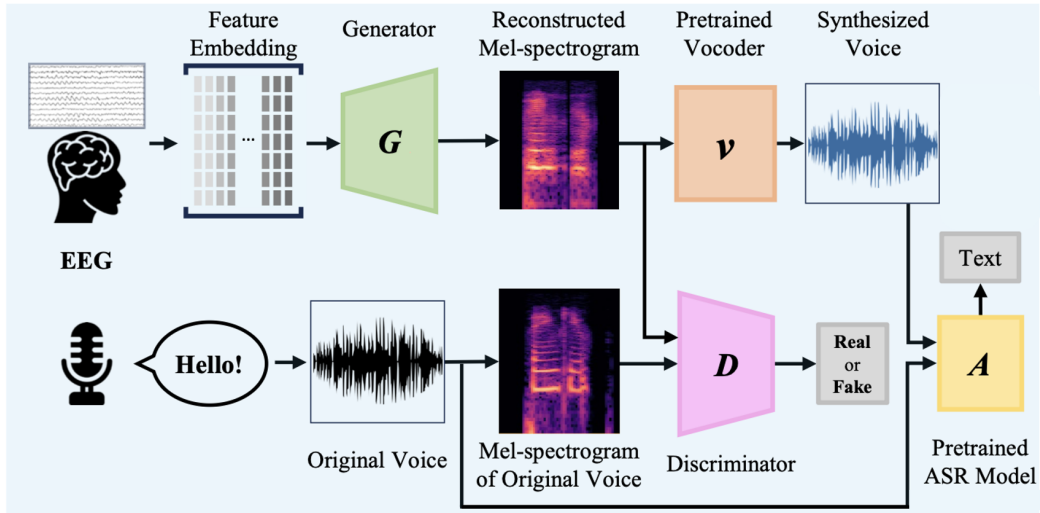


Figure 16: Overall framework for EEG to speech synthesis (Park et al., 2024): G denotes the generator, which maps EEG embeddings to mel-spectrograms; D is the discriminator that compares real and generated mel-spectrograms; V is a pre-trained vocoder that converts mel-spectrograms into audio waveforms; and A is a pre-trained ASR model for speech-to-text conversion.

2021; Ramirez-Aristizabal and Kello, 2022; Park et al., 2024; Mizuno et al., 2024; Postolache et al., 2024; Jiang et al., 2024; Lee et al., 2024, 2025), others explore speaking tasks and imagined speech (Krishna et al., 2021; Lee et al., 2023b,a; Xiong et al., 2025).

For more naturalistic communication, Lee et al. (2023b) convert EEG signals recorded during imagined speech into the user’s own voice, enabling **personalized speech synthesis**. Similarly, Park et al. (2024) generate speech from EEG while simultaneously producing a synchronized talking face with accurate lip movements.

For **speech decoding from listened speech**, Lee et al. (2024) propose an end-to-end framework that directly reconstructs natural speech waveforms from non-invasive EEG recorded while subjects listen to closed-vocabulary sentences. In a related work, the same authors Lee et al. (2025) extend this framework with a BiLSTM based phoneme predictor that outputs decoded phoneme sequences in the text modality, enabling listened speech to be reconstructed in both modalities: speech waveforms and textual phoneme sequences.

These studies address **key challenges**, including the generation of fragmented or abstract outputs (Park et al., 2024), the difficulty of synthesizing complete and continuous speech from EEG (Mizuno et al., 2024), the limitation of music reconstruction to relatively simple compositions with limited timbres (Postolache et al., 2024), the lack of standardized vocabularies for aligning EEG with audio data (Jiang et al., 2024) and bypassing the dependency on intermediate acoustic feature mappings such as mel-spectrograms (Lee et al., 2024).

5.5. Generative Architectures Used Across Studies

EEG-to-speech and EEG-to-audio generation builds on a range of modeling and representation learning approaches. As we highlighted before, a prominent strategy is to leverage the shared signal modality between EEG and audio by mapping

both into a **common intermediate representation, such as a mel-spectrogram**.

We now outline the major state-of-the-art techniques for EEG-to-speech generation, highlighting the underlying approaches of each method and their relevance.

- **Convolutional Neural Network (CNN)-based models** have been widely employed to generate audio waveforms from EEG input (Krishna et al., 2021; Ramirez-Aristizabal and Kello, 2022). Krishna et al. (2021) propose a CNN architecture comprising temporal convolution layers, 1D convolutional layers, and a time-distributed layer to synthesize audio waveforms directly from EEG recorded during both speaking and listening tasks. Similarly, Ramirez-Aristizabal and Kello (2022) use sequential CNN regressors to reconstruct music stimuli by mapping EEG features to mel-spectrogram representations.
- **Recurrent Neural Networks (RNNs)-based models**, particularly GRUs and LSTMs, have been used for sequential EEG encoding in speech reconstruction tasks. In the NeuroTalk framework, Lee et al. (2023b) employ a **GRU-based generator to produce mel-spectrograms from imagined-speech EEG**, which are then converted into waveforms using the HiFi-GAN **vocoder** (Kong et al., 2020) and transcribed into text using HuBERT (Hsu et al., 2021), a self-supervised speech representation model. Building on this framework, Park et al. (2024) extend EEG-based speech synthesis by integrating synchronized talking-face generation, leveraging Wave2Lip (Prajwal et al., 2020) and Apple’s Avatar API to achieve accurate lip synchronization with synthesized speech.
- **Transformers and latent diffusion models** have recently been adopted to **capture long-range dependencies and improve audio reconstruction quality**. Mizuno et al.

EEG-to-Audio/Speech Generation Evaluation Metrics			
Category	Metric	Description / Usage in Studies	References
Signal-based	MCD	Mel Cepstral Distortion; quantifies spectral distortion between generated and reference speech waveforms.	Krishna et al. (2021); Park et al. (2024); Lee et al. (2024, 2025)
	RMSE	Root Mean Square Error; measures average squared deviation between reconstructed and original signals.	Krishna et al. (2021); Park et al. (2024)
Spectrogram similarity	SSIM	Structural Similarity Index; assesses perceptual similarity between generated and ground-truth spectrograms.	Ramirez-Aristizabal and Kello (2022)
	PSNR	Peak Signal-to-Noise Ratio; evaluates spectrogram reconstruction clarity and fidelity.	Ramirez-Aristizabal and Kello (2022)
Linguistic accuracy	WER	Word Error Rate; percentage of word-level errors indicating intelligibility of reconstructed speech.	Mizuno et al. (2024)
	CER	Character Error Rate; character-level transcription accuracy for fine-grained evaluation.	Mizuno et al. (2024)
	BERTScore	Embedding-based semantic similarity for transcripts derived from reconstructed speech.	Mizuno et al. (2024)
Perceptual quality	FAD	Fréchet Audio Distance; compares feature distributions of real and generated audio for perceptual similarity.	Postolache et al. (2024)
Subjective task-specific	MOS	Mean Opinion Score; listener-based subjective rating of audio naturalness and quality.	Lee et al. (2023b)
	Hits@k	Retrieval relevance metric for task-based evaluation (e.g., search/classification).	Jiang et al. (2024)

Table 4: Evaluation metrics used in EEG-to-audio/speech generation studies.

(2024) employ transformer-based architectures for EEG-to-speech reconstruction, while Jiang et al. (2024) use a transformer encoder **to generate emotive music from EEG signals**. In the domain of naturalistic music decoding, Postolache et al. (2024) integrate EEG features with AudioLDM2 (Liu et al., 2024b), a pre-trained latent diffusion model, guided by a ControlNet adapter (Zhang et al., 2023) to achieve controllable and high-quality music generation.

5.6. EEG Feature Encoding and Representation

Feature encoding determines how neural signals are transformed into intermediate acoustic representations or directly mapped into audio features. Existing studies employ a variety of strategies, including the extraction of articulatory and acoustic features, temporal feature encoding, and the use of mel-spectrograms as shared representations.

Articulatory and acoustic features provide an interpretable bridge between EEG signals and speech outputs. Krishna et al. (2021) incorporate an attention model to predict articulatory features from EEG activity and an attention-regression model to convert these into acoustic features for waveform synthesis.

Temporal feature encoding has also been explored as a pathway to represent EEG dynamics for speech and music generation. Jiang et al. (2024) derive EEG tokens through a multi-step process that includes DBSCAN clustering to extract temporal features, which are then augmented with positional encoding to yield structured EEG tokens that can be used in downstream decoding tasks.

Mel-spectrograms provide a shared latent space between EEG and audio signals and thereby facilitating cross-modal translation. Ramirez-Aristizabal and Kello (2022) employ a sequential CNN regressor to map EEG signals directly to time-aligned music spectrograms and Xiong et al. (2025) employ a CNN-GRU based decoder to convert learned EEG latent representation to mel-spectrograms.

In a related approach, Lee et al. (2023a) adapt spoken EEG into the subspace of imagined EEG by applying **Common Spatial Pattern (CSP) filters** trained on imagined speech, capturing temporal oscillatory patterns and reducing distributional differences between spoken and imagined EEG to enable user-specific voice synthesis. Similarly, Postolache et al. (2024) apply CSP filtering while temporally aligning EEG with speech, using triggers to mark onset intervals and segment continuous brain signals into utterance-specific intervals.

5.7. Evaluation Metrics

Evaluation of EEG-to-speech generation relies on established speech and audio metrics that **assess similarity to reference signals, intelligibility, perceptual quality, and subjective human judgments**. These can be broadly grouped into signal-based metrics, spectrogram similarity metrics, linguistic accuracy metrics, perceptual quality metrics, and subjective assessments. Table 4 lists the key evaluation metrics with brief descriptions and exemplary studies that have used them.

6. Limitations and Future Work

This section outlines the major limitations observed across all modalities and explores potential directions for advancing the field by addressing these challenges and leveraging the gaps identified in existing studies.

1. **ML features vs. EEG-domain features.** In existing studies, temporal and spatial EEG features are typically extracted using machine-learning architectures such as CNNs and autoregressive sequence models. However, these learned representations are rarely compared with **traditional EEG-domain features**, including time-domain waveform oscillations, Event-Related Potentials (ERPs), or phase-synchronization indices. Establishing a **comparison between ML-derived features and neuroscience-informed EEG features**, or integrating EEG-domain features to guide or augment the generative process, remains an open and promising direction for future research.
2. **Embedding based features lack cognitive intuitiveness.** Most current EEG-to-media models rely on embedding-based representations learned by deep networks, but these features are difficult to interpret and offer limited insight into the underlying cognitive processes. This **lack of interpretability reduces our ability to connect model representations with established neuroscientific knowledge** and hinders trust in the decoding pipeline. There is a need to integrate principles from cognitive psychology and neuroscience to design features that more directly reflect brain activity. Additionally, emerging ML interpretability techniques could be leveraged to map embedding-based representations onto cognitive processes and improve the transparency of generative models.
3. **Algorithm Optimization.** Although some studies explore multimodal fusion, this area remains largely underdeveloped. **Advancing multimodal fusion strategies and designing EEG-specific deep learning frameworks** could lead to more effective modeling of how the brain processes information across different modalities. Such optimized architectures may better capture the complementary relationships between EEG signals and visual, auditory, or linguistic stimuli, ultimately improving the quality and robustness of EEG-to-media generation.
4. **Laboratory vs. Real-world experiments.** Laboratory environments provide controlled conditions for EEG acquisition, but real-world settings are far more complex and variable. Real-life environments introduce numerous factors, such as environmental noise, unpredictable stimuli, and natural variations in images, text, and audio, that are difficult to replicate or simulate in controlled laboratory studies. As a result, **models trained exclusively on lab data may lack ecological validity**. Incorporating real-world multimodal EEG datasets, or combining real-world recordings with laboratory studies, could lead to more robust models and improve the generalizability and trustworthiness of EEG-to-media generation systems.
5. **Inherent limitations of EEG.** EEG suffers from a **relatively low signal-to-noise ratio**, which poses challenges for reliably capturing fine-grained neural information. Although recent work has shown promising progress in generating media from EEG, combining EEG with other physiological signals, such as functional near-infrared spectroscopy (fNIRS), could help overcome these limitations. Moreover, **EEG primarily captures cortical surface activity, with limited sensitivity to subcortical structures** that play crucial roles in auditory, emotional, and temporal processing. As a result, EEG-to-media generation models rely mostly on cortical correlates and may miss important subcortical contributions, particularly for tasks such as speech reconstruction or auditory decoding. Integrating EEG with complementary modalities that better capture subcortical dynamics (e.g., fNIRS, MEG, or auditory brainstem responses) could provide richer neural representations and improve generation quality.
6. **Lack of standardized benchmarks.** A key challenge is that there are currently no standardized paradigms for conducting EEG-to-media studies, including consistent protocols for data collection, data splitting strategies, datasets, feature extraction methods, generative model architectures, or evaluation metrics. As a result, comparing results across studies is difficult, and it becomes challenging to trace how generation performance has evolved over time. Establishing standardized baselines, such as shared datasets, reference frameworks, and evaluation metrics, would enable more reliable comparisons, improve reproducibility, and support systematic progress in future research.

7. Conclusion

With rapid progress in machine learning, generative AI in particular, EEG is emerging as a viable foundation for cross-modal generation, including text, image, and speech synthesis directly from brain signals. Despite persistent challenges such as low signal-to-noise ratio and limited spatial resolution, this growing research area demonstrates a meaningful shift toward more ambitious, non-invasive brain-computer interface (BCI) capabilities.

In this survey, we reviewed the landscape of EEG-based generative AI research across text, image, and audio domains, highlighting representative use cases, datasets, generative frameworks, and open challenges. We provided a comprehensive synthesis of methods employed in EEG-driven generative tasks, summarizing major datasets and the core model architectures adopted across the surveyed studies. To ground these developments, we also included foundational background on generative modeling and an overview of the neural basis through which EEG reflects perceptual and cognitive activity elicited by different types of stimuli. In addition, we identified key limitations of existing work, including small and heterogeneous datasets, low signal fidelity, limited cross-subject generalization, and the need for more interpretable and neurally aligned generative frameworks.

Progress in this field will require the development of standardized benchmarks with consistent data splits, preprocessing pipelines, and evaluation metrics. Such standardization would improve reproducibility, enable fairer comparisons, and help clarify which methodological innovations genuinely advance performance. Ethical considerations, including privacy, informed consent, and responsible use of neural data, should remain central as research continues to evolve.

Overall, while EEG-driven generative AI remains an emerging and highly experimental area, continued research, supported by better datasets, unified evaluation practices, and deeper integration with neuroscientific principles, is essential for advancing understanding and expanding the scope of what non-invasive neural decoding can achieve.

References

- Ahmadiéh, H., Gassemi, F., Moradi, M.H., 2024. Visual image reconstruction based on eeg signals using a generative adversarial and deep fuzzy neural network. *Biomedical Signal Processing and Control* 87, 105497.
- Alharbi, Y.F., Alotaibi, Y.A., 2024. Decoding imagined speech from eeg data: A hybrid deep learning approach to capturing spatial and temporal features. *Life* 14, 1501.
- Amrani, H., Micucci, D., Napoletano, P., 2024. Deep representation learning for open vocabulary electroencephalography-to-text decoding. *IEEE Journal of Biomedical and Health Informatics*.
- Bai, Y., Wang, X., Cao, Y.p., Ge, Y., Yuan, C., Shan, Y., 2023. Dreamdiffusion: Generating high-quality images from brain eeg signals. *arXiv preprint arXiv:2306.16934*.
- Banerjee, S., Lavie, A., 2005. Meteor: An automatic metric for mt evaluation with improved correlation with human judgments, in: *Proceedings of the acl workshop on intrinsic and extrinsic evaluation measures for machine translation and/or summarization*, pp. 65–72.
- Bastiaansen, M., Hagoort, P., 2006. Oscillatory neuronal dynamics during language comprehension. *Progress in brain research* 159, 179–196.
- Bastiaansen, M.C., Oostenveld, R., Jensen, O., Hagoort, P., 2008. I see what you mean: theta power increases are involved in the retrieval of lexical semantic information. *Brain and language* 106, 15–28.
- Bastiaansen, M.C., Van Berkum, J.J., Hagoort, P., 2002. Event-related theta power increases in the human eeg during online sentence processing. *Neuroscience letters* 323, 13–16.
- Bengio, Y., Ducharme, R., Vincent, P., Jauvin, C., 2003. A neural probabilistic language model. *Journal of machine learning research* 3, 1137–1155.
- Bhattasali, S., Brennan, J., Luh, W.M., Franzluebbers, B., Hale, J., 2020. The alice datasets: fmri & eeg observations of natural language comprehension, in: *Proceedings of the Twelfth Language Resources and Evaluation Conference*, pp. 120–125.
- Biswal, S., Xiao, C., Westover, M.B., Sun, J., 2019. Eegto-text: learning to write medical reports from eeg recordings, in: *Machine Learning for Healthcare Conference, PMLR*. pp. 513–531.
- Bria, A., Marrocco, C., Tortorella, F., 2021. Sinc-based convolutional neural networks for eeg-bci-based motor imagery classification, in: *International Conference on Pattern Recognition, Springer*. pp. 526–535.
- Broderick, M.P., Anderson, A.J., Lalor, E.C., 2019. Semantic context enhances the early auditory encoding of natural speech. *Journal of Neuroscience* 39, 7564–7575.
- Chen, Q., Wang, Y., Wang, F., Sun, D., Li, Q., 2025. Decoding text from electroencephalography signals: A novel hierarchical gated recurrent unit with masked residual attention mechanism. *Engineering Applications of Artificial Intelligence* 139, 109615.
- Cheng, W., Tan, J., Wang, L., Herrero, M.T., Zeng, H., 2025. Fine-grained image generation with eeg multi-level semantics. *Computer Methods and Programs in Biomedicine*, 108909.
- Demiralp, T., Bayraktaroglu, Z., Lenz, D., Junge, S., Busch, N.A., Maess, B., Ergen, M., Herrmann, C.S., 2007. Gamma amplitudes are coupled to theta phase in human eeg during visual perception. *International journal of psychophysiology* 64, 24–30.
- Di, G.Q., Fan, M.C., Lin, Q.H., 2018. An experimental study on eeg characteristics induced by intermittent pure tone stimuli at different frequencies. *Applied Acoustics* 141, 46–53.
- Duan, Y., Zhou, J., Wang, Z., Wang, Y.K., Lin, C.T., 2023. Dewave: Discrete eeg waves encoding for brain dynamics to text translation. *arXiv preprint arXiv:2309.14030*.
- Fahimi Hnazaee, M., Khachatryan, E., Van Hulle, M.M., 2018. Semantic features reveal different networks during word processing: An eeg source localization study. *Frontiers in human neuroscience* 12, 503.
- Farahani, E.D., Wouters, J., van Wieringen, A., 2021. Brain mapping of auditory steady-state responses: A broad view of cortical and subcortical sources. *Human brain mapping* 42, 780–796.
- Feng, X., Feng, X., Qin, B., Liu, T., 2023. Aligning semantic in brain and language: A curriculum contrastive method for electroencephalography-to-text generation. *IEEE Transactions on Neural Systems and Rehabilitation Engineering*.

- Gedawy, M.E., Nabil, O., Mamdouh, O., Nady, M., Adel, N.A., Fares, A., 2025. Bridging brain signals and language: A deep learning approach to eeg-to-text decoding. *arXiv preprint arXiv:2502.17465* .
- Goodfellow, I., Pouget-Abadie, J., Mirza, M., Xu, B., Warde-Farley, D., Ozair, S., Courville, A., Bengio, Y., 2020. Generative adversarial networks. *Communications of the ACM* 63, 139–144.
- Grootswagers, T., Zhou, I., Robinson, A.K., Hebart, M.N., Carlson, T.A., 2022. Human eeg recordings for 1,854 concepts presented in rapid serial visual presentation streams. *Scientific Data* 9, 3.
- Guenther, S., Kosmyrna, N., Maes, P., 2024. Image classification and reconstruction from low-density eeg. *Scientific Reports* 14, 16436.
- Haarmann, H.J., Cameron, K.A., Ruchkin, D.S., 2002. Neural synchronization mediates on-line sentence processing: Eeg coherence evidence from filler-gap constructions. *Psychophysiology* 39, 820–825.
- Hagoort, P., Hald, L., Bastiaansen, M., Petersson, K.M., 2004. Integration of word meaning and world knowledge in language comprehension. *science* 304, 438–441.
- Herdman, A.T., Lins, O., Van Roon, P., Stapells, D.R., Scherg, M., Picton, T.W., 2002. Intracerebral sources of human auditory steady-state responses. *Brain topography* 15, 69–86.
- Ho, J., Jain, A., Abbeel, P., 2020. Denoising diffusion probabilistic models. *Advances in neural information processing systems* 33, 6840–6851.
- Hollenstein, N., Rotsztein, J., Troendle, M., Pedroni, A., Zhang, C., Langer, N., 2018. Zuco, a simultaneous eeg and eye-tracking resource for natural sentence reading. *Scientific data* 5, 1–13.
- Hollenstein, N., Troendle, M., Zhang, C., Langer, N., 2019. Zuco 2.0: A dataset of physiological recordings during natural reading and annotation. *arXiv preprint arXiv:1912.00903* .
- Hsu, W.N., Bolte, B., Tsai, Y.H.H., Lakhotia, K., Salakhutdinov, R., Mohamed, A., 2021. Hubert: Self-supervised speech representation learning by masked prediction of hidden units. *IEEE/ACM transactions on audio, speech, and language processing* 29, 3451–3460.
- Ikegawa, Y., Fukuma, R., Sugano, H., Oshino, S., Tani, N., Tamura, K., Iimura, Y., Suzuki, H., Yamamoto, S., Fujita, Y., et al., 2024. Text and image generation from intracranial electroencephalography using an embedding space for text and images. *Journal of Neural Engineering* 21, 036019.
- Jiang, H., Chen, Y., Wu, D., Yan, J., 2024. Eeg-driven automatic generation of emotive music based on transformer. *Frontiers in Neurorobotics* 18, 1437737.
- Jiang, X., Zhou, C., Duan, Y., Zhao, Z., Do, T., Lin, C.T., 2025. Neural spelling: A spell-based bci system for language neural decoding. *arXiv preprint arXiv:2501.17489* .
- Kaneshiro, B., Nguyen, D.T., Dmochowski, J.P., Norcia, A.M., Berger, J., 2016. Naturalistic music eeg dataset—hindi (nmed-h). *Stanford Digital Repository*.
- Kaneshiro, B., Perreau Guimaraes, M., Kim, H.S., Norcia, A.M., Suppes, P., 2015. A representational similarity analysis of the dynamics of object processing using single-trial eeg classification. *Plos one* 10, e0135697.
- Kavasidis, I., Palazzo, S., Spampinato, C., Giordano, D., Shah, M., 2017. Brain2image: Converting brain signals into images, in: *Proceedings of the 25th ACM international conference on Multimedia*, pp. 1809–1817.
- Khadir, A., Maghareh, M., Sasani Ghamsari, S., Beigzadeh, B., 2023. Brain activity characteristics of rgb stimulus: an eeg study. *Scientific Reports* 13, 18988.
- Khaleghi, N., Rezaii, T.Y., Beheshti, S., Meshgini, S., Sheykhivand, S., Danishvar, S., 2022. Visual saliency and image reconstruction from eeg signals via an effective geometric deep network-based generative adversarial network. *Electronics* 11, 3637.
- Kingma, D.P., Welling, M., et al., 2019. An introduction to variational autoencoders. *Foundations and Trends® in Machine Learning* 12, 307–392.
- Kong, J., Kim, J., Bae, J., 2020. Hifi-gan: Generative adversarial networks for efficient and high fidelity speech synthesis. *Advances in neural information processing systems* 33, 17022–17033.
- Krause, C.M., Lang, A.H., Laine, M., Kuusisto, M., Pörn, B., 1996. Event-related. eeg desynchronization and synchronization during an auditory memory task. *Electroencephalography and clinical neurophysiology* 98, 319–326.
- Krause, C.M., Pörn, B., Lang, A.H., Laine, M., 1997. Relative alpha desynchronization and synchronization during speech perception. *Cognitive brain research* 5, 295–299.
- Krishna, G., Tran, C., Carnahan, M., Tewfik, A.H., 2021. Advancing speech synthesis using eeg, in: *2021 10th International IEEE/EMBS Conference on Neural Engineering (NER)*, IEEE. pp. 199–204.
- Kumar, P., Saini, R., Roy, P.P., Sahu, P.K., Dogra, D.P., 2018. Envisioned speech recognition using eeg sensors. *Personal and Ubiquitous Computing* 22, 185–199.
- Lan, Y.T., Ren, K., Wang, Y., Zheng, W.L., Li, D., Lu, B.L., Qiu, L., 2023. Seeing through the brain: Image reconstruction of visual perception from human brain signals. *arXiv e-prints* , arXiv–2308.

- Lawhern, V.J., Solon, A.J., Waytowich, N.R., Gordon, S.M., Hung, C.P., Lance, B.J., 2018. Eegnet: a compact convolutional neural network for eeg-based brain-computer interfaces. *Journal of neural engineering* 15, 056013.
- Lee, J., Feng, T., Kommineni, A., Kadiri, S.R., Narayanan, S., 2025. Enhancing listened speech decoding from eeg via parallel phoneme sequence prediction, in: *ICASSP 2025-2025 IEEE International Conference on Acoustics, Speech and Signal Processing (ICASSP)*, IEEE. pp. 1–5.
- Lee, J., Kommineni, A., Feng, T., Avramidis, K., Shi, X., Kadiri, S., Narayanan, S., 2024. Toward fully-end-to-end listened speech decoding from eeg signals. *arXiv preprint arXiv:2406.08644* .
- Lee, Y.E., Kim, S.H., Lee, S.H., Lee, J.S., Kim, S., Lee, S.W., 2023a. Speech synthesis from brain signals based on generative model, in: *2023 11th International Winter Conference on Brain-Computer Interface (BCI)*, IEEE. pp. 1–4.
- Lee, Y.E., Lee, S.H., Kim, S.H., Lee, S.W., 2023b. Towards voice reconstruction from eeg during imagined speech, in: *Proceedings of the AAAI Conference on Artificial Intelligence*, pp. 6030–6038.
- Li, D., Du, C., He, H., 2020. Semi-supervised cross-modal image generation with generative adversarial networks. *Pattern Recognition* 100, 107085.
- Li, D., Wei, C., Li, S., Zou, J., Qin, H., Liu, Q., 2024. Visual decoding and reconstruction via eeg embeddings with guided diffusion. *arXiv preprint arXiv:2403.07721* .
- Lin, C.Y., 2004. Rouge: A package for automatic evaluation of summaries, in: *Text summarization branches out*, pp. 74–81.
- Liu, H., Hajjaligol, D., Antony, B., Han, A., Wang, X., 2024a. Eeg2text: Open vocabulary eeg-to-text decoding with eeg pre-training and multi-view transformer. *arXiv preprint arXiv:2405.02165* .
- Liu, H., Yuan, Y., Liu, X., Mei, X., Kong, Q., Tian, Q., Wang, Y., Wang, W., Wang, Y., Plumbley, M.D., 2024b. Audioldm 2: Learning holistic audio generation with self-supervised pretraining. *IEEE/ACM Transactions on Audio, Speech, and Language Processing* .
- Liu, X., Shen, D., Liu, X., 2025. Learning interpretable representations leads to semantically faithful eeg-to-text generation. *arXiv preprint arXiv:2505.17099* .
- Lopez, E., Sigillo, L., Colonnese, F., Panella, M., Comminiello, D., 2025. Guess what i think: Streamlined eeg-to-image generation with latent diffusion models, in: *ICASSP 2025-2025 IEEE International Conference on Acoustics, Speech and Signal Processing (ICASSP)*, IEEE. pp. 1–5.
- Losorelli, S., Nguyen, D.T., Dmochowski, J.P., Kaneshiro, B., 2017. Nmed-t: A tempo-focused dataset of cortical and behavioral responses to naturalistic music., in: *ISMIR*, p. 5.
- Lu, J.T.Y., Chiang, J., Chen, C.S., Tung, A.N.Y., Hu, H.W., Cheng, Y.C., 2025. Eeg2text-cn: An exploratory study of open-vocabulary chinese text-eeg alignment via large language model and contrastive learning on chinese eeg. *arXiv preprint arXiv:2506.00854* .
- Lutzenberger, W., Pulvermüller, F., Elbert, T., Birbaumer, N., 1995. Visual stimulation alters local 40-hz responses in humans: an eeg-study. *Neuroscience letters* 183, 39–42.
- Marinković, K., 2004. Spatiotemporal dynamics of word processing in the human cortex. *The Neuroscientist* 10, 142–152.
- Masry, M., Amen, M., Elzyat, M., Hamed, M., Magdy, N., Khaled, M., 2025. Ets: Open vocabulary electroencephalography-to-text decoding and sentiment classification. *arXiv preprint arXiv:2506.14783* .
- Mehmood, T., Ahmad, H., Shakeel, M.H., Taj, M., 2025. Catvis: Context-aware thought visualization, in: *International Conference on Medical Image Computing and Computer-Assisted Intervention*, Springer. pp. 98–108.
- Mishra, A., Shukla, S., Torres, J., Gwizdka, J., Roychowdhury, S., 2024. Thought2text: Text generation from eeg signal using large language models (llms). *arXiv preprint arXiv:2410.07507* .
- Mishra, R., Sharma, K., Jha, R.R., Bhavsar, A., 2023. Neurogan: image reconstruction from eeg signals via an attention-based gan. *Neural Computing and Applications* 35, 9181–9192.
- Mizuno, T., Kishida, T., Yoshimura, N., Nakashika, T., 2024. An investigation on the speech recovery from eeg signals using transformer, in: *2024 Asia Pacific Signal and Information Processing Association Annual Summit and Conference (APSIPA ASC)*, IEEE. pp. 1–6.
- Nemrodov, D., Niemeier, M., Patel, A., Nestor, A., 2018. The neural dynamics of facial identity processing: insights from eeg-based pattern analysis and image reconstruction.
- Odena, A., Buckman, J., Olsson, C., Brown, T., Olah, C., Raffel, C., Goodfellow, I., 2018. Is generator conditioning causally related to gan performance?, in: *International conference on machine learning*, PMLR. pp. 3849–3858.
- Orima, T., Motoyoshi, I., 2021. Analysis and synthesis of natural texture perception from visual evoked potentials. *Frontiers in Neuroscience* 15, 698940.
- Palazzo, S., Spampinato, C., Kavasidis, I., Giordano, D., Schmidt, J., Shah, M., 2020. Decoding brain representations by multimodal learning of neural activity and visual features. *IEEE Transactions on Pattern Analysis and Machine Intelligence* 43, 3833–3849.

- Papineni, K., Roukos, S., Ward, T., Zhu, W.J., 2002. Bleu: a method for automatic evaluation of machine translation, in: Proceedings of the 40th annual meeting of the Association for Computational Linguistics, pp. 311–318.
- Park, J.H., Lee, S.H., Lee, S.W., 2024. Towards eeg-based talking-face generation for brain signal-driven dynamic communication, in: 2024 46th Annual International Conference of the IEEE Engineering in Medicine and Biology Society (EMBC), IEEE. pp. 1–5.
- Pfurtscheller, G., Neuper, C., Mohl, W., 1994. Event-related desynchronization (erd) during visual processing. *International journal of psychophysiology* 16, 147–153.
- Postolache, E., Polouliakh, N., Kitano, H., Connelly, A., Rodolà, E., Cosmo, L., Akama, T., 2024. Naturalistic music decoding from eeg data via latent diffusion models. arXiv preprint arXiv:2405.09062 .
- Prajwal, K., Mukhopadhyay, R., Namboodiri, V.P., Jawahar, C., 2020. A lip sync expert is all you need for speech to lip generation in the wild, in: Proceedings of the 28th ACM international conference on multimedia, pp. 484–492.
- Ramirez-Aristizabal, A.G., Kello, C., 2022. Eeg2mel: Reconstructing sound from brain responses to music. arXiv preprint arXiv:2207.13845 .
- Rathod, V.S., Tiwari, A., Kakde, O.G., 2024. Folded ensemble deep learning based text generation on the brain signal. *Multimedia Tools and Applications* , 1–29.
- Rezvani, A., Akbari, A., Arani, K.S., Mirian, M., Arasteh, E., McKeown, M.J., 2025. Interpretable eeg-to-image generation with semantic prompts. arXiv preprint arXiv:2507.07157 .
- Salimans, T., Goodfellow, I., Zaremba, W., Cheung, V., Radford, A., Chen, X., 2016. Improved techniques for training gans. *Advances in neural information processing systems* 29.
- Sellam, T., Das, D., Parikh, A.P., 2020. Bleurt: Learning robust metrics for text generation. arXiv preprint arXiv:2004.04696 .
- Shimizu, H., Srinivasan, R., 2022. Improving classification and reconstruction of imagined images from eeg signals. *biorxiv*. retrieved july 5, 2022.
- Singh, P., Dalal, D., Vashishtha, G., Miyapuram, K., Raman, S., 2024. Learning robust deep visual representations from eeg brain recordings, in: Proceedings of the IEEE/CVF Winter Conference on Applications of Computer Vision, pp. 7553–7562.
- Singh, P., Pandey, P., Miyapuram, K., Raman, S., 2023. Eeg2image: image reconstruction from eeg brain signals, in: ICASSP 2023-2023 IEEE International Conference on Acoustics, Speech and Signal Processing (ICASSP), IEEE. pp. 1–5.
- Song, Y., Liu, B., Li, X., Shi, N., Wang, Y., Gao, X., 2023. Decoding natural images from eeg for object recognition. arXiv preprint arXiv:2308.13234 .
- Spampinato, C., Palazzo, S., Kavasidis, I., Giordano, D., Souly, N., Shah, M., 2017. Deep learning human mind for automated visual classification, in: Proceedings of the IEEE conference on computer vision and pattern recognition, pp. 6809–6817.
- Srivastava, A., Shinde, T., 2020. Think2type: Thoughts to text using eeg waves. *International Journal of Engineering Research & Technology (IJERT)* 9, 2278–018.
- Sugimoto, Y., Pongthaisorn, G., Capi, G., 2024. Image generation using eeg data: A contrastive learning based approach, in: 2024 IEEE Canadian Conference on Electrical and Computer Engineering (CCECE), IEEE. pp. 794–798.
- Tao, Y., Liang, Y., Wang, L., Li, Y., Yang, Q., Zhang, H., 2024. See: Semantically aligned eeg-to-text translation. arXiv preprint arXiv:2409.16312 .
- Tirupattur, P., Rawat, Y.S., Spampinato, C., Shah, M., 2018. Thoughtviz: Visualizing human thoughts using generative adversarial network, in: Proceedings of the 26th ACM international conference on Multimedia, pp. 950–958.
- Toffolo, K.K., Freedman, E.G., Foxe, J.J., 2022. Evoking the n400 event-related potential (erp) component using a publicly available novel set of sentences with semantically incongruent or congruent eggplants (endings). *Neuroscience* 501, 143–158.
- Vaswani, A., Shazeer, N., Parmar, N., Uszkoreit, J., Jones, L., Gomez, A.N., Kaiser, Ł., Polosukhin, I., 2017. Attention is all you need. *Advances in neural information processing systems* 30.
- Wakita, S., Orima, T., Motoyoshi, I., 2021. Photorealistic reconstruction of visual texture from eeg signals. *Frontiers in Computational Neuroscience* 15, 754587.
- Wang, J., Song, Z., Ma, Z., Qiu, X., Zhang, M., Zhang, Z., 2024. Enhancing eeg-to-text decoding through transferable representations from pre-trained contrastive eeg-text masked autoencoder. arXiv preprint arXiv:2402.17433 .
- Wang, Z., Ji, H., 2022. Open vocabulary electroencephalography-to-text decoding and zero-shot sentiment classification, in: Proceedings of the AAAI Conference on Artificial Intelligence, pp. 5350–5358.
- Weiss, S., Mueller, H.M., 2003. The contribution of eeg coherence to the investigation of language. *Brain and language* 85, 325–343.
- Weiss, S., Mueller, H.M., 2012. “too many betas do not spoil the broth”: the role of beta brain oscillations in language processing. *Frontiers in psychology* 3, 201.

- Weiss, S., Mueller, H.M., Schack, B., King, J.W., Kutas, M., Rappelsberger, P., 2005. Increased neuronal communication accompanying sentence comprehension. *International journal of psychophysiology* 57, 129–141.
- Wolpaw, J.R., Boulay, C.B., 2010. Brain signals for brain–computer interfaces, in: *Brain-Computer Interfaces: Revolutionizing Human-Computer Interaction*. Springer, pp. 29–46.
- Xiong, W., Ma, L., Li, H., 2025. Synthesizing intelligible utterances from eeg of imagined speech. *Frontiers in Neuroscience* 19, 1565848.
- Xu, J., Aristimunha, B., Feucht, M.E., Qian, E., Liu, C., Shahjahan, T., Spyra, M., Zhang, S.Z., Short, N., Kim, J., et al., 2024. Alljoined—a dataset for eeg-to-image decoding. *arXiv preprint arXiv:2404.05553*.
- Yang, J., Awais, M., Hossain, M.A., Yee, L., Haowei, M., Mehedi, I.M., Iskanderani, A., 2023a. Thoughts of brain eeg signal-to-text conversion using weighted feature fusion-based multiscale dilated adaptive densenet with attention mechanism. *Biomedical Signal Processing and Control* 86, 105120.
- Yang, L., Zhang, Z., Song, Y., Hong, S., Xu, R., Zhao, Y., Zhang, W., Cui, B., Yang, M.H., 2023b. Diffusion models: A comprehensive survey of methods and applications. *ACM computing surveys* 56, 1–39.
- Yu-Hao Chen, T., Chen, Y., Soederhaell, P., Agrawal, S., Shapovalenko, K., 2025. Decoding eeg speech perception with transformers and vae-based data augmentation. *arXiv e-prints*, arXiv–2501.
- Zander, T.O., Kothe, C., Jatzev, S., Gaertner, M., 2010. Enhancing human-computer interaction with input from active and passive brain-computer interfaces. *Brain-computer interfaces: Applying our minds to human-computer interaction*, 181–199.
- Zeng, H., Xia, N., Qian, D., Hattori, M., Wang, C., Kong, W., 2023a. Dm-re2i: A framework based on diffusion model for the reconstruction from eeg to image. *Biomedical Signal Processing and Control* 86, 105125.
- Zeng, H., Xia, N., Tao, M., Pan, D., Zheng, H., Wang, C., Xu, F., Zakaria, W., Dai, G., 2023b. Dcae: A dual conditional autoencoder framework for the reconstruction from eeg into image. *Biomedical Signal Processing and Control* 81, 104440.
- Zhang, H., Goodfellow, I., Metaxas, D., Odena, A., 2019a. Self-attention generative adversarial networks, in: *International conference on machine learning*, PMLR. pp. 7354–7363.
- Zhang, L., Rao, A., Agrawala, M., 2023. Adding conditional control to text-to-image diffusion models, in: *Proceedings of the IEEE/CVF International Conference on Computer Vision*, pp. 3836–3847.
- Zhang, T., Kishore, V., Wu, F., Weinberger, K.Q., Artzi, Y., 2019b. Bertscore: Evaluating text generation with bert. *arXiv preprint arXiv:1904.09675*.
- Zhang, Z., Ding, X., Bao, Y., Zhao, Y., Liang, X., Qin, B., Liu, T., 2024. Chisco: An eeg-based bci dataset for decoding of imagined speech. *Scientific Data* 11, 1265.
- Zhao, S., Rudzicz, F., 2015. Classifying phonological categories in imagined and articulated speech, in: *2015 IEEE international conference on acoustics, speech and signal processing (ICASSP)*, IEEE. pp. 992–996.

Appendix A. Baseline Datasets and Implementations

In this section, we summarize key datasets, one for each modality, previously described in the modality-specific subsections, together with reference resources for recommended baseline architectures used to generate images, text, and audio from EEG signals. Our aim is to provide researchers with a clear starting point by presenting both widely used open-source datasets and representative baseline models for each modality.

Appendix A.1. EEG-to-Image

Key resources: EEG-Based Visual Classification dataset [Spampinato et al. \(2017\)](#); [Palazzo et al. \(2020\)](#) and EEG encoder framework for Brain2Image [Kavasidis et al. \(2017\)](#).

Dataset: The EEG-Based Visual Classification dataset contains 128-channel EEG recordings from 6 subjects while viewing images from the ImageNet dataset. Stimuli comprised 40 object classes with 50 images per class, for a total of 2,000 images. Dataset is publicly available at [this link](#).

EEG encoder framework: An open-source repository of LSTM- and deep neural network (DNN)-based EEG encoders, primarily developed for visual classification tasks from EEG signals. Code implementation is available at [this link](#).

Appendix A.2. EEG-to-Text

Key resources: Zurich Cognitive Language Processing Corpus 2.0 (ZuCo 2.0) dataset [Hollenstein et al. \(2019\)](#); EEG-to-Text sequence-to-sequence decoding framework leveraging pre-trained language models (e.g., BART) [Wang and Ji \(2022\)](#).

Dataset: The ZuCo 2.0 dataset provides multimodal recordings of eye gaze and 128-channel EEG brain activity from 18 participants. Subjects read a stimulus set of 739 English sentences, including 349 in a normal reading paradigm and 390 in a task-specific paradigm. Dataset is publicly available at [this link](#).

EEG-to-Text decoding framework: An open-source sequence-to-sequence framework for decoding EEG signals into text, leveraging pre-trained language models such as BART. Code implementation is available at [this link](#).

Appendix A.3. EEG-to-Audio

Key resources: KARA One dataset [Zhao and Rudzicz \(2015\)](#); Voice reconstruction framework from EEG during imagined speech using mel-spectrograms as intermediate representations [Lee et al. \(2023b\)](#).

Dataset: The KARA One dataset provides multimodal recordings from 8 participants across three modalities: 64-channel EEG, facial motion, and audio. Data were collected during both imagined and vocalized phonemic and single-word prompts. Dataset is publicly available at [this link](#).

EEG-to-Speech synthesis framework: The EEG-to-speech synthesis framework leverages mel-spectrograms as an intermediate representation. It comprises (i) a generator that maps EEG embeddings to mel-spectrograms, (ii) a discriminator that evaluates real versus generated spectrograms, and (iii) a vocoder that converts mel-spectrograms into audio waveforms. Code implementation is available at [this link](#).

We further encourage future work to adopt these suggested baselines to facilitate meaningful performance comparisons across architectures, thereby enabling more systematic and reproducible progress in generative modeling from EEG signals.